RECOVERY OF AMMONIA FROM SIMULATED MEMBRANE CONTACTOR EFFLUENT USING BIPOLAR MEMBRANE ELECTRODIALYSIS

by

DAVID SAABAS

B.A.Sc, University of British Columbia/University of Northern British Columbia, 2014

A THESIS SUBMITTED IN PARTIAL FULFILLMENT OF
THE REQUIREMENTS FOR THE DEGREE OF

MASTER OF APPLIED SCIENCE

in

THE FACULTY OF GRADUATE AND POSTDOCTORAL STUDIES

(Civil Engineering)

THE UNIVERSITY OF BRITISH COLUMBIA

(Vancouver)

August 2021

The following individuals certify that they have read, and recommend to the Faculty of Graduate and Postdoctoral Studies for acceptance, the thesis entitled:

Recovery of ammonia from simulated membrane contactor effluent using bipolar membrane electrodialysis

submitted by David Saabas in partial fulfillment of the

the degree of Master of Applied Science

in Civil Engineering

Examining Committee:

Jongho Lee, Civil Engineering, UBC

Supervisor

Simcha Srebnik, Chemical and Biological Engineering, UBC

Additional Examiner

Abstract

Abundant in municipal, agricultural, and industrial wastewaters, ammonia is a versatile chemical, which can be used as fertilizer or as a hydrogen carrier for the hydrogen economy. Membrane contactors (MC) are an effective membrane process for selectively recovering ammonia from a wastewater stream, but the system's continuous acid consumption and the residual acidity in the produced stream remain a major hurdle. In this study, we propose a chemical-free, electrified process that combines MC with bipolar membrane electrodialysis (BMED) to produce ammonia as a gas from wastewater. We devise three different BMED configurations, and identify the most suitable configuration by examining the impact of different operating conditions including pH, initial ammonia concentration, and relative volume ratios on the ammonia recovery and BMED energy consumption. We demonstrate up to ~68% recovery of theoretically recoverable ammonia, and attribute the unrecovered fraction primarily to the diffusion of neutral ammonia through membranes. While the system is sub-optimal, the relative energy consumption of the system is comparable to the Haber-Bosch process for conventional ammonia production, with potentially lower energy consumption and higher ammonia recovery through higher initial ammonia concentrations, higher relative volume ratios or alternate BMED configurations.

Lay Summary

Ammonia is a chemical often present in wastewater that is toxic to humans and aquatic life and therefore often converted into nitrogen gas at wastewater treatment plants. However, ammonia is also a versatile chemical that can be used as a fertilizer or a hydrogen fuel carrier. Membrane contactors (MC) are an effective process for selectively recovering ammonia from wastewater but they consume acid while operating. Bipolar membrane electrodialysis (BMED) is another process used for ammonia recovery, but this process generates acid as a byproduct of ammonia recovery. We combine these two processes to recovery ammonia and recycle acid between the MC and BMED processes. We demonstrate that this process is feasible and can generate recover ammonia from wastewater with energy consumption similar to industrial ammonia production.

Preface

The research is conducted in UBC's Environment Laboratory by the author, David Saabas, under the supervision of Dr. Jongho Lee.

Table of Contents

List of Tables

List of Figures

List of Equations

List of Abbreviations

AAS	Atomic absorption spectroscopy
AEM	Anion-exchange membrane
BMED	Bipolar membrane electrodialysis
BPM	Bipolar membrane
CEM	Cation-exchange membrane
FIA	Flow injection analysis
IEM	Ion-exchange membrane
MC	Membrane contactor
PFD	Process flow diagram
TAN	Total ammonia nitrogen

List of Symbols

I_t	Current at time i (A)
M	Concentration of ion in (mol L^{-1})
t	Elapsed time in experiment (s)
Δt	Time between current measurements (s)
V_{stack}	Potential difference between stack anode and cathode (V)

Acknowledgements

I would like to thank my supervisor, Dr. Jongho Lee, for his support, ideas and advice, both in research and in academics, throughout my degree.

I would like to thank my colleagues Abhishek Dutta, Hiroki Fukuda, and Sifat Kalam for their support in the lab, and Abhishek again for teaching me about membrane contactors.

I also acknowledge the funding support from the Natural Sciences and Engineering Research Council of Canada (NSERC) through a GCS-M Grant.

Dedication

For my family

1 Introduction

Wastewater treatment has always been important to preserve public health and protect receiving water bodies from pollution, but wastewater is increasingly being seen as a potential source of resources as opposed to merely a waste product [1], [2]. Many wastewater treatment plants recover entrained carbon as methane through anaerobic digestion to produce energy, but there has not been widespread adoption of nutrient recovery [3]. Nitrogen compounds in wastewater, such as nitrates, nitrites, and ammonia are toxic to humans and to aquatic life. In wastewater treatment plants that practice nutrient removal, ammonia is typically treated using the nitrification-denitrification process that converts ammonia to nitrogen gas [1], [2], [4]. While this process is environmentally benign, it prevents this potential resource from being recovered [2].

Ammonia is a versatile chemical that can be used as a fertilizer, a fuel, or as a potential hydrogen carrier [1], [4], [5]. It is estimated that ammonia entrained in wastewater equates to ~19% of global ammonia production [1]. Nitrogen based fertilizers are available in many different forms including anhydrous ammonia (NH_3), urea, ammonium salts, and ammonia solutions. As the densest form of ammonia, anhydrous ammonia is used as a feedstock to produce other nitrogen-based fertilizers [6], [7]. The Haber-Bosch process, which combines methane and nitrogen gas to create NH_3, is dominantly employed for anhydrous ammonia production. Due to the high demand of nitrogen-based fertilizers, the process accounts for ~1-2% of energy consumption worldwide [1], [4], [8]. Ammonia also has potential to act as a hydrogen carrier as liquid ammonia is more energy efficient to transport than liquid hydrogen, even when the energy associated with converting ammonia back to hydrogen is considered [5], [9]. While methane recovery from wastewater treatment plants has been pursued, ~40% of the chemical energy present in wastewater is in the form of ammonia, not organic carbon [1]. As the demand for nitrogen-based fertilizer is increasing around the world [10] and hydrogen fuel cells are gaining traction, particularly in the Asian market [9], ammonia entrained in wastewater represents a potential carbon-free ammonia source.

Membrane contactors (MC) are a viable method of recovering ammonia from wastewater and a number of studies have demonstrated selective ammonia removal and high ammonia recoveries ranging from ~84-99% [4], [11]–[14]. Briefly, MC systems introduce ammonia-containing wastewater into the feed side of a hydrophobic porous membrane, and an acidic solution on the draw side of the membrane. The air bubbles trapped in the membrane pores allow only gasses to

pass through the membrane. The acid-base reaction between ammonia and the acid in the draw solution results in a very low partial pressure of ammonia gas in the membrane-draw solution interface, creating a partial pressure gradient of ammonia gas in the membrane pores and driving the gas from the feed to the draw side [15]. The transferred ammonia then forms an ammonium salt in the draw solution [15].

A simplified process flow diagram of the MC is shown in Figure 1A. The ammonia recovery by MC is a spontaneous process. In addition, the ammonia-selective mechanism makes MC effluent generally free from many other contaminants in the wastewater, such as non-volatile organics and dissolved compounds [13]. However, some MC processes for ammonia recovery typically use excess acid in the draw solution and in all cases, MC systems consume acid to recover ammonia. If excess acid is used, the resulting ammonium salt in the draw solution cannot be directly used as fertilizer, because most crops are not tolerant of acidic environments. Even if the resulting product is of neutral pH, acid is continuously consumed by the MC and ammonium salts are less valuable as fertilizer than anhydrous ammonia [16], [17].

To avoid chemical consumption and generate a more valuable product, NH_3, bipolar membrane electrodialysis (BMED) can be used as a post-processing step for the MC. As a variant of electrodialysis, BMED is an electrochemical process that is commonly used for the production of acids and bases from salts [18], [19]. A BMED “Stack” consists of layers of flow compartments, anion exchange membranes (AEM), cation exchange membranes (CEM), and bipolar membranes (BPM). An AEM (or CEM) is embedded with positively (or negatively) charged groups, allowing anions (or cations) to pass through the membrane. A BPM consists of an AEM and a CEM that are fused together, and therefore prevent any charged molecules from passing through the membrane. Under a potential difference applied across the anode and cathode, water inside the BPM is split into H^+ (proton) and OH^- (hydroxide), generating acid and base [18]. Ammonia recovery from real and simulated wastewaters using BMED has been demonstrated in previous studies [4], [20]–[23]. However, many of the processes described in the BMED studies produce a dilute effluent stream and an acid stream without an immediate use. Furthermore, while the transport of other ions present in wastewater only accounted for a slight decrease in current efficiency, membrane fouling issues could exist with long term operation in BMED systems exposed to wastewater [4].

The BMED and MC processes complement each other for the purposes of extracting ammonia from wastewater. The MC can protect the ion exchange membranes (IEMs) in the BMED system by acting as a barrier against non-volatile organics and other ions present in the wastewater [13] and the BMED system regenerates acid to be recycled back to the MC. The product from this combined system is ammonia (gas), which is more versatile chemical and more commonly used as fertilizer than ammonium salts [17]. Further, this process eliminates the consumption of acid by the MC and allows for electrification of nutrient recovery, promoting sustainable wastewater treatment where energy grids are decarbonizing.

In this paper, we devise BMED processes for ammonia gas production as a post-treatment system of a MC, without generating liquid waste streams and without chemical consumption. Specifically, three different configurations are investigated: 2-compartment BMED with a separate base loop and CEMs, 2-compartment BMED with a split flow loop and CEMs, and 2-compartment BMED with split flow loop and AEMs. For each configuration, we examine the impact of MC effluent composition and the operating conditions on the ammonia recovery performance. Based on the ammonia recovery and energy consumption, we identify the most suitable BMED system configuration for integration with a MC. Finally, potential approaches for process improvement are discussed. Our study demonstrates the potential of a combined MC-BMED system to recover ammonia and reduce chemical consumption associated with MC systems. If renewable electricity is used, ammonia entrained in wastewater can be recovered without carbon emissions for use as a fertilizer or a fuel.

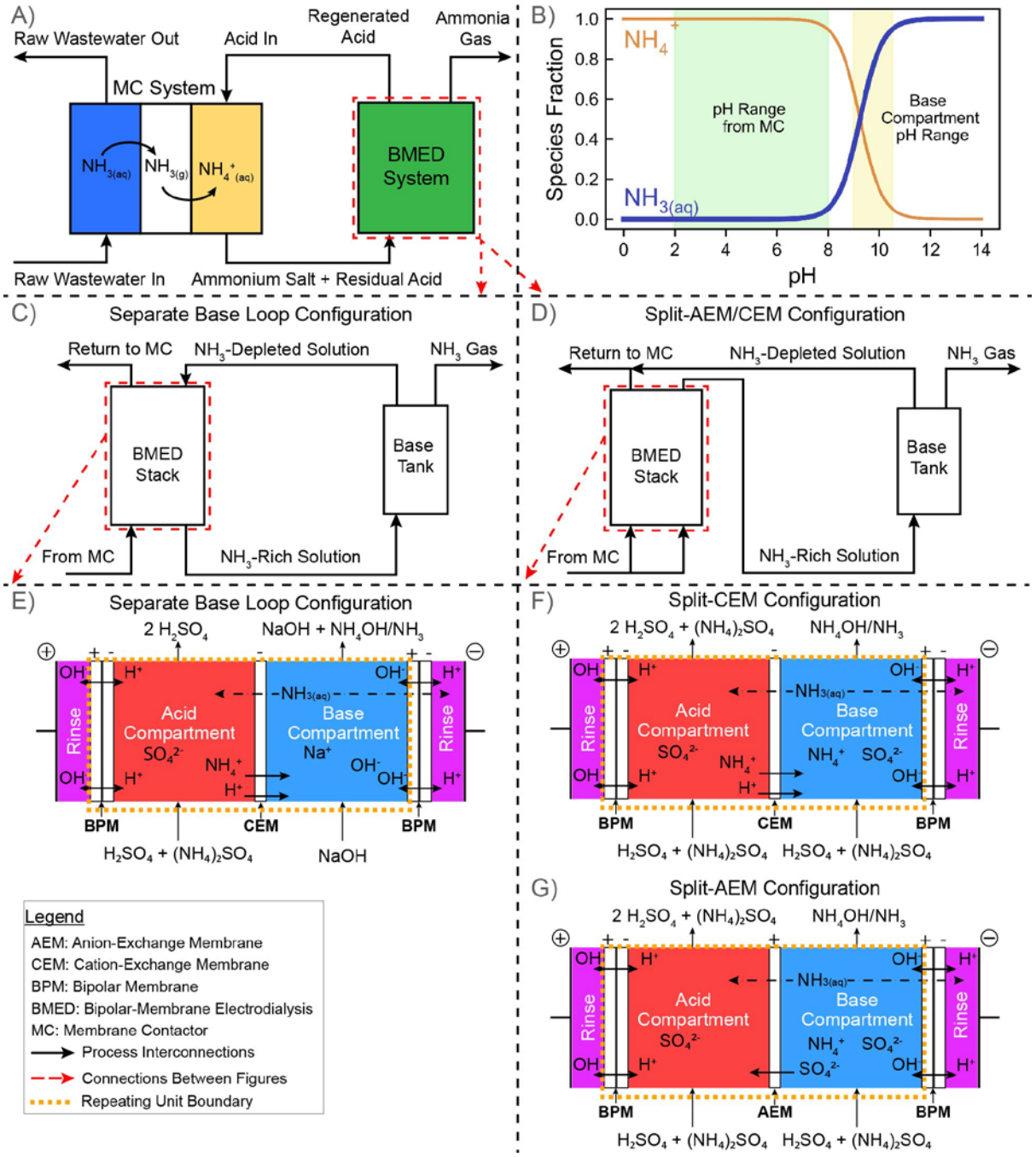

Figure 1: (A) Process schematic combining MC and BMED for gas ammonia production from wastewater. (B) NH_3/NH_4^+ equilibrium diagram showing the expected pH range of MC effluent and BMED base compartment. (C) Process flow diagram of BMED system with separate base loop. (D) Process flow diagram of BMED system with split flow coming from the MC. Schematic illustrations of ionic flows for (E) separate base loop (SBL) configuration, (F) split-CEM configuration, and (G) split-AEM configuration of BMED system.

2 Materials and Methods

2.1 BMED system configurations

In order to integrate the BMED process with a MC as shown in Figure 1A, the combined system should meet the following objectives: (1) recovery of NH_3 as a gas; (2) regeneration of acid for its recirculation into the MC; (3) closed-loop operation as to not generate a liquid waste stream. In solution ammonia can either exist in an ionic form, NH_4^+, or as a dissolved gas, NH_3. The equilibrium between these two ammonia species is dictated by the solution pH as described in Equation 1. The sum of both dissolved NH_3 and NH_4^+ in solution is referred to as total ammonia nitrogen (TAN).

Equation 1: Ammonia/Ammonium Equilibrium

$$NH_4^+{}_{(aq)} \rightleftarrows NH_{3(aq)} + H^+{}_{(aq)} \qquad pKa = 9.25 \tag{1}$$

The BMED stack generates acid and base streams. The low pH of the acid stream returned to the MC would maintain the ammonia species in the MC effluent predominantly as NH_4^+, while NH_3 gas can be extracted from the base stream (Figure 1B).

Three BMED configurations capable of achieving these objectives were tested, all of which use a 2-compartment membrane layout. The first configuration uses a separate base loop (SBL), where the circulating base fluid is separated from the MC effluent by a CEM. In the SBL configuration (Figure 1C), 100% of the MC effluent is passed through the acid compartment of the BMED stack. Illustrated in Figure 1D, the second and third configurations split MC effluent flow into the acid and base compartments, separated by CEMs (split-CEM configuration) and AEMs (split-AEM configuration), respectively. For both configurations, the flow streams exiting the acid and base compartments are mixed back together before being returned to the MC. In all configurations, there were three repeating cell units, and the rinse compartments that are in direct contact with the electrodes were separated from the acid and base compartments with BPMs. All experiments were carried out at a constant 8V potential difference between electrodes.

2.1.1 Separate Base Loop Configuration

The membrane layout for the SBL configuration is shown in Figure 1E. In this configuration, cations in the acid compartment are replaced with protons during operation (i.e., M^+/H^+ substitution) [18], [24]. The cations are mobile in the BMED stack and migrate toward the cathode from one compartment to another. The anions in the system remain in their initial compartment as they are blocked from reaching the next compartment by a CEM. The base side of the system is filled with 0.01M NaOH solution to maintain compartment conductivity and high pH [23]. The acid compartment is filled with a solution containing ammonium sulfate ($(NH_4)_2SO_4$) and sulfuric acid (H_2SO_4). As NH_4^+ migrates toward the cathode from the acid compartment to the base compartment, the sufficiently high pH of the base compartment (~pH 12 initially due to NaOH concentration) leads to conversion of NH_4^+ into dissolved NH_3 gas which can then be extracted. An NH_4^+ ion removed from the acid compartment is replaced with a proton that is generated by the BPM. This proton addition regenerates H_2SO_4 in the acid compartment, which will then be returned to the MC. The rinse compartment is filled 0.4 M sodium sulfate (Na_2SO_4).

2.1.2 Split Configuration – CEM

The membrane layout for the split-CEM configuration is shown in Figure 1F. This configuration also uses the M^+/H^+ substitution. In this system, NH_4^+ ions that migrate from the acid into the base compartment are counterbalanced by the hydroxide ions generated by the BPM, which increases the pH inside the base compartment and therefore results in formation of dissolved NH_3 gas. The pH of the acid compartment decreases due to the replacement of NH_4^+ ions with protons generated by BPM. When NH_4^+ ions in the base compartment are converted to NH_3 gas, the pH of the base compartment decreases as the proton from NH_4^+ neutralizes the hydroxide in solution [21]. Therefore, when the acid and base solutions are mixed back together before being returned to the MC system, there will be a net increase in the number of protons of the BMED effluent relative to its influent, regenerating the acid for the MC.

2.1.3 Split Configuration – AEM

The membrane layout for the split-AEM configuration is shown in Figure 1G. Contrary to the previous configurations, this configuration uses the X^-/OH^- substitution [18], [24]; the sulfate ions (SO_4^{2-}) in the base compartment migrate to the acid compartment and are replaced with hydroxide

ions from the BPM. The SO_4^{2-} then becomes the counter-ion for protons generated by the BPM in the acid compartment. The cations in the system remain in their initial compartment as they are prevented from travelling to the cathode by the AEM. Above pH 4, nearly 100% of sulfate species exist as SO_4^{2-}, leaving the concentration of HSO_4^- negligible. The pH in the base compartment increases as SO_4^{2-} ions are replaced with hydroxide ions generated by the BPM. The pH in the acid compartment decreases as protons are generated by the BPM to balance the charge of the SO_4^{2-} ions entering the acid compartment. As the pH of the base compartment increases, NH_4^+ ions in the base compartment are again converted to NH_3 gas. This conversion decreases the pH of the base compartment and there will therefore be a net increase in the number of protons once the acid and base streams are mixed back together and returned to the MC.

2.2 Experimental Setup and Procedure

A process flow diagram (PFD) of the laboratory setup is shown in Figure 2. The experiment is operated as a semi-batch process where the acid, base, and rinse solutions are recirculated and the acid bottle and base tank are continuously stirred. This can partially simulate plug flow in a larger BMED system with a larger number of stacks and a greater membrane area. The gas extraction system on the base tank operates continuously. The capture system is included in order to measure the captured NH_3, as was done in previous studies[23]. The suction side of a vacuum pump is connected to the headspaces of the base tank and the capture tank, and the discharge is connected to diffusion fittings submerged in the solution of both tanks. This method dissolves NH_3 gas from the headspace of the base tank into the acidic capture solution, preserving it for analysis as NH_4^+. Headspace gasses are circulated through the two tanks to agitate the base tank fluid, which facilitates ammonia transfer. The details of the experimental setup are included in Appendix A, and mechanical drawings of the BMED stack are included in Appendix B. The total ammonia recovery is calculated as the ratio of the mass of TAN in the capture solution to the TAN of the entire system, as described in Equation 2:

Equation 2: Ammonia Recovery Calculation

$$Recovery = \frac{TAN\ Mass\ in\ Capture\ Solution}{Total\ System\ TAN\ Mass} \quad (2)$$

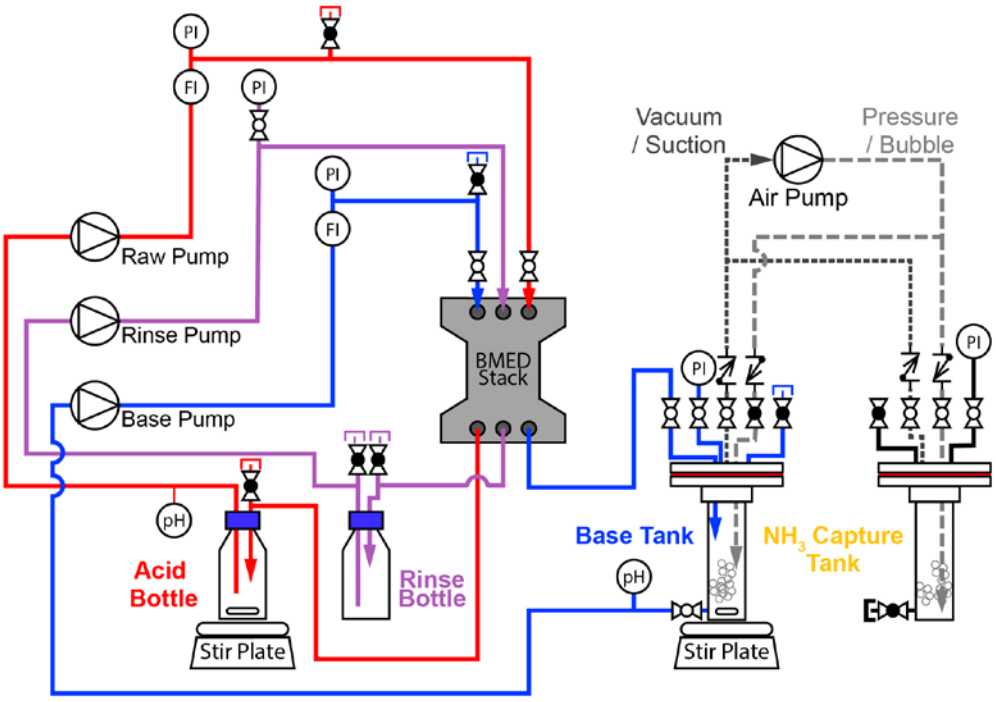

Figure 2: The experimental setup used in the lab for 2-compartment BMED configuration testing. The NH_3 capture tank is not hydraulically connected to the rest of the process but is placed to re-dissolve ammonia that has been extracted from the base tank for TAN measurement. PI, FI, and pH in the diagram indicate pressure gauge, flow indicator, and pH meter, respectively.

As a neutral species, NH_3 diffuses into the rinse compartment over time as shown in Figure 1E,F,G [18], [19], [25]. As the TAN concentration increases in the rinse compartment, the pH increases and equilibrium promotes formation of NH_3 gas, which increases the pressure inside the rinse bottle. As a result, the circulating pressure of the rinse compartment may exceed the circulating pressure of the acid and base compartments. In such a case, rinse solution can leak into the other compartments, contaminate the acid and base streams, and increase the system current. To mediate this pressurization of the rinse solution, a 0.5 psi pressure-relief valve was added to the headspace of the rinse bottle. Based on the mass balance analysis, the amount of NH_3 lost through this pressure relief valve was found to be negligible.

2.3 Membranes and Electrodes

The specifications of membrane used in our study are shown in Table 1. The membranes were then cut to fit into the BMED stack (150mm x 65mm). Holes were then punched into the membranes for the flow channels within the stack. The active area of each membrane was 25 cm^2. Stainless steel 316 Plates (150mm x 65mm x 3.175mm) were used for both anode and cathode.

Table 1. Membrane Specifications

Membrane	Manufacturer	Thickness (um)	Areal Resistance (Ω cm^2)	Selectivity	Water Splitting Efficiency
FBM Bipolar Membrane	Fumatech	130-160	-	-	>98%*
FAS-PK-130 Anion Exchange Membrane	Fumatech	115-138	< 4	>95%	-
FAB-PK-130 Anion Exchange Membrane	Fumatech	126-140	3.27	98%	-

*Water splitting efficiency at 100 mA/cm^2

2.4 Solution Preparation

For this experiment, we are attempting to mimic the composition of the effluent of a MC that treats ammonia-containing wastewater. With an acidic draw solution (commonly sulfuric acid), MC effluent primarily contains ammonium salt and residual acid. TAN concentrations in MC effluent can vary from ~1,000 mg/L-N to ~10,000 mg/L-N with the effluent pH ranging 2-8 [11], [12], [26], [27]. Since ammonia concentrations in wastewater used in MC studies is typically in the range of ~1000-4000 ppm-N [11]–[13], [27], in our experiment we make the conservative assumption that the MC is a “pass-through” device and does not concentrate the ammonia. In our experiments a baseline ammonia concentration of 2000 mg/L-N was used, and the effluent pH was assumed to be between 2 and 8, with a baseline pH of 5.

Four solutions were prepared for the experiment, three to circulate through the acid, base, rinse compartments, and one solution in the capture system. The acid solution was prepared using ≥99.0% ACS, VWR Chemicals BDH ammonium sulfate, dissolving 9.43 g (for a 2000 ppm-N) into 1 L of distilled water, then by adding 50 µL of 0.1 M sulfuric acid to obtain pH 5. Excess acid was added for low-pH experiments and Sigma Aldrich 35% Ammonia Solution was used to adjust the raw solution to pH 8.

In the SBL configuration, the prepared acid solution was only used in the acid compartment, while in the split-AEM and -CEM membrane configurations, the same solution was used in both acid and base compartments. In the SBL configuration, a 0.01M solution of NaOH in distilled water was used in the base compartment. For all configurations, the rinse compartment was 0.4 M Sigma Aldrich >99% sodium sulfate, and the capture solution was 400 mL of distilled water with 4 mL of Sigma Aldrich 95-98% sulfuric acid. Excess acid was added to the capture solution to ensure that nearly 100% of the recovered TAN existed as NH_4^+. For the SBL experiments, the acid compartment volume was 1.2 L and the base compartment volume was 0.4 L. In the split-AEM and CEM equal volumes of acid and base, ~0.425L, were used unless otherwise indicated.

2.5 Chemical Analysis

Samples were taken from the circulating acid, base, and rinse solutions using a luer-lock syringe from an in-line sample port. The capture solution was sampled directly from the tank as there is no circulating fluid. Ammonia concentrations were measured as TAN using flow injection analysis (FIA) (Lachat Instruments QuikChem FIA+ 8000 Series). TAN samples used a 201x dilution in pH 2.5 H_2SO_4. Sodium concentrations were measured using atomic absorption spectroscopy (AAS) (Varian SpectrAA 220). Sodium samples were diluted in 2000 ppm-K KCl solution as per AAS procedure: 11x dilution for acid and base samples, and 5001x dilution for the rinse solution was performed.

3 Results and Discussion

3.1 Separate Base Loop Configuration

Figure 3 presents the overall performance of the SBL configuration. In principle, as NH_4^+ crosses the CEM into the base compartment, the charge would be balanced by a hydroxide ion generated by the BPM in the base compartment. Accordingly, the high pH in the base compartment quickly converts NH_4^+ to NH_3, and the proton neutralizes the hydroxide, maintaining a steady pH [22], [26]. As shown in Figure 3A, however, we observed a consistent drop in the base compartment pH during first 5 hours of the experiment, from ~12 to ~10.5. This pH drop corresponded to the decreasing system current from ~200 mA to ~40 mA (Figure 3B). The system current is carried by the movement of ions through the BMED stack [19]. In a 2 compartment BMED system using CEM membranes, protons also migrate from the acid compartment to the base compartment. As a proton migrates out of the acid compartment, it is replaced with a proton generated by the BPM. This newly generated proton will migrate toward the cathode under the influence of the potential gradient, and the cycle will repeat. This continuous stream of protons accounts for a portion of the total system current and reduces current efficiency [28], that is, the ratio of current used for NH_4^+ transport compared to the total system current [19]. The decrease in system current indicates that transmembrane flux of NH_4^+ from acid to base compartments has also decreased, leading to a low ammonia recovery performance. At the 5-hour mark of the experiment, a 5 mL dose of 5M NaOH was added to the base tank. This intervention immediately increased the base tank pH and the system current. However, the system current and base tank pH continued to decrease over the remainder of the 19-hour experiment (not shown in Figure 3A). The base solution pH returned to ~10 by hour 19 of the experiment.

The Na^+ concentration in the base compartment decreased over time, corresponding to an increase in the acid compartment Na^+ concentration. There were no losses of Na^+ from the rinse compartment during the experiment. The Na^+ concentration in the base compartment increased with the addition of NaOH. The data suggest that Na^+ ions were migrating against the potential gradient, which will be discussed in the following section. This trend was observed in multiple SBL configuration experiments.

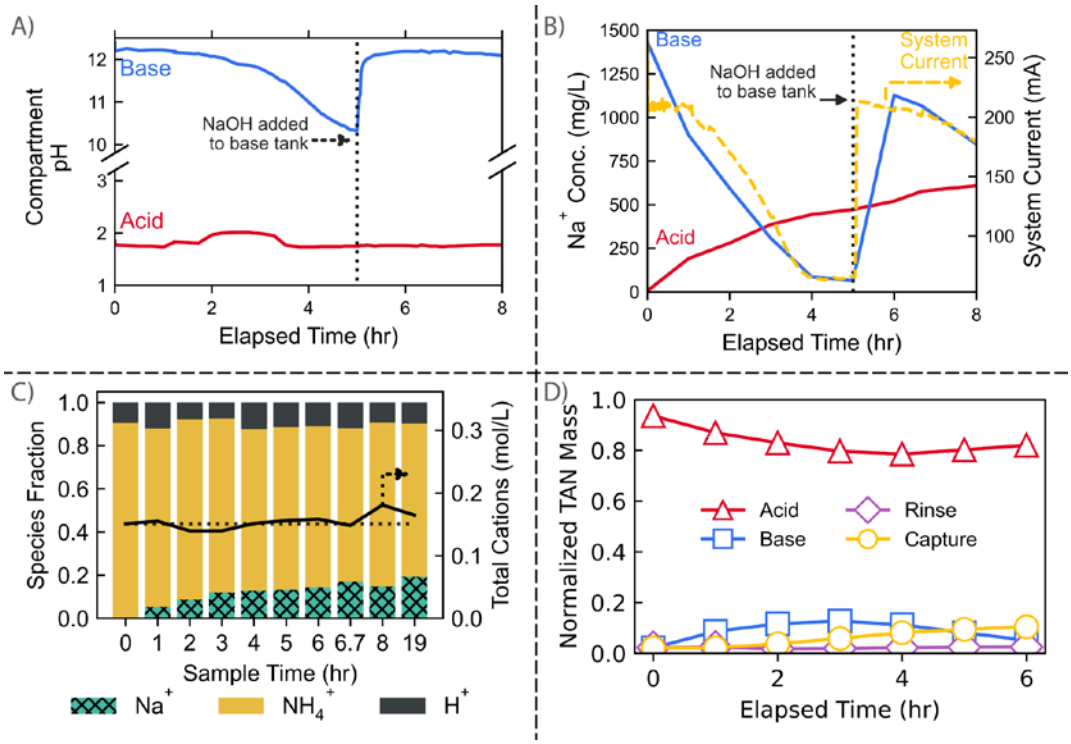

Figure 3: System performance of separate base loop BMED configuration. (A) pH in each compartment over the course of the experiment, where sodium hydroxide was added at 5 hrs. (B) Sodium ion concentration in each compartment and system current over time. Sodium hydroxide was added to the base compartment at 5hrs. (C) Cationic balance and molar fractions in the acid compartment over the course of the experiment. Constant cation concentration indicates that membranes were working as expected. The dotted line indicates the initial cation concentration. (D) TAN masses in each compartment normalized to TAN mass in the system.

3.1.1 Cation Balance

The underlying cause of the decreasing pH in the base compartment and the system current was further examined by analyzing the cation balance in the acid compartment. The constant volumes of acid and base tanks confirm that there is no fluid leakage between the different compartments across membranes. To ensure the stack was operating correctly, the system was troubleshooted as described in Appendix A.

As is shown in Figure 1E, anions theoretically cannot leave the acid compartment as a CEM prevents them from travelling toward the anode. Therefore, there must be a constant number of positive counter-ions to the sulfate that is in solution. When a cation migrates out of the acid

compartment, it is replaced by a proton. The total cation concentration was calculated using Equation 3.

Equation 3: Cation Balance in the Acid Compartment for a 2-Compartment CEM Configuration

$$\sum_{i}^{n}[Cation_i]_{(M)} = [Na^+]_{(M)} + [NH_4^+]_{(M)} + [H^+]_{(M)} \quad (3)$$

A representative cation balance of the acid compartment for the SBL is shown in Figure 3C. The total cation balance remained relatively constant over the course of the experiment. However, the fraction of Na^+ in the acid compartment was steadily increasing with time, implying that Na^+ migrates against the electrical potential. If a fluid leak was responsible for the sodium infiltration, we would expect to see an increase in the total cation concentration. It appears that protons from the acid compartment were replacing Na^+ ions in the base compartment, which could be explained by an order of magnitude higher mobility of protons relative to all other cations via the proton-tunneling mechanism [19] (Table 2). Migration of Na^+ ions against the potential gradient, while not violating the overall charge balance, has been observed in ion-separation electrodialysis experiments and frequently observed in Donnan dialysis [29], [30].

Table 2. Diffusion coefficients and mobility coefficients for species in experimental system [31]

Species	Diffusion Coefficient [m^2/s]	Mobility [m^2mol/Js]
H^+	$9.30x10^{-9}$	$3.75x10^{-12}$
NH_4^+	$1.95x10^{-9}$	$7.89x10^{-13}$
Na^+	$1.33x10^{-9}$	$5.37x10^{-13}$
OH^-	$5.25x10^{-9}$	$2.12x10^{-12}$
SO_4^{2-}	$1.06x10^{-9}$	$4.28x10^{-12}$

This phenomenon would explain the observed pH and system current trends. The excessive proton migration into the base compartment decreases the pH due to the neutralization of protons and hydroxide ions. In addition, as the Na^+ concentration in the base compartment decreases, the conductivity of the cell decreases, which will increase the resistance of the stack and decrease the system current when operating at a constant voltage.

It is possible that due to the high H^+ concentration in the acid compartment, it is less energetically demanding for the BMED system to maintain electroneutrality by displacing a Na^+ ion from the base compartment with a high-mobility proton migrating from the acid compartment than for the BPM to split water to generate a new hydroxide counterion. The depletion of Na^+ ions from the base solution results in three undesirable effects: (1) the base solution loses conductivity and therefore increases the resistance of the stack, (2) the pH of the base solution decreases, making ammonia extraction more difficult, and (3) the BMED system "consumes" NaOH which is contrary to the overall goal of reducing chemical consumption. The accumulation of Na^+ ions in the acid stream could potentially "contaminate" the solution circulating through the MC-BMED system.

3.1.2 Ammonia Recovery

The amount of ammonia in each compartment is compared based on the TAN mass in the compartment normalized to the TAN mass of the whole system, which allows us to obtain the relative ammonia recovery and is defined as:

Equation 4: Normalized TAN mass

$$Normalized\ TAN\ Mass = \frac{TAN\ Mass\ in\ Compartment_i}{TAN\ Mass\ in\ System} \quad (4)$$

The normalized TAN concentration for each compartment is shown in Figure 3D. There was an initial increase in the TAN concentration in the base compartment, reaching a maximum value at ~3 hours. Even after the addition of NaOH to the base compartment to restore stack conductivity, the TAN concentration in the base compartment decreased and the TAN concentration in the acid compartment remained constant. The TAN leaving the base compartment is transferred as

ammonia gas to the capture tank, from which approximately 10% of the ammonia species in the total system was recovered. While this SBL configuration is relatively simple and features a separate loop of base solution (e.g., NaOH), the reverse migration of Na^+ causes the system to consume chemicals, in the form of base, and not reliably recover ammonia.

3.2 Split-CEM Configuration

As shown in Figure 1D, both split-CEM and –AEM configurations split the feed (i.e., MC effluent) into the acid and base compartments, without a separate NaOH base loop. The normalized TAN concentration in each compartment over the course of the experiment is shown in Figure 4A. Even after >20 hours of operation, there was little ammonia recovery in the capture solution, ~14%. There was an initial increase in concentration in the base compartment due to the incoming NH_4^+ ions crossing the CEM. Afterwards, the NH_4^+ concentration gradually decreased for the remainder of the experiment as the NH_4^+ was recovered as NH_3 gas. The low recovery can be explained by the low base compartment pH, seen in Figure 4B. However, the recovery from this system configuration is limited by the initial solution pH and the relative volume split of the MC effluent between the acid and base compartments. This is due to the neutralization that will occur in the base compartment as NH_3 is removed. The NH_3 that is present in the base compartment at the beginning of the experiment is predominantly present as NH_4^+ ion. At a feed pH of 8, the highest considered in this study, 95% of the TAN are present as NH_4^+. At pH 2 and 5, the fraction of TAN present as NH_4^+ approaches 100%. The hydroxide ions generated by the BPM are stoichiometrically limited by the NH_4^+ ions crossing the CEM into the base compartment. The pH in the base compartment increases as NH_4^+ ions enter the base compartment and decreases as hydroxide ions are neutralized by the conversion of NH_4^+ to NH_3. Therefore, the NH_3 starting in the base compartment cannot be removed. Any protons that cross the CEM will be neutralized by the hydroxide ions generated by the BPM in the base compartment.

Initially, the base compartment pH quickly increases to a maximum value of ~8.5, then gradually decreases for the remainder of the experiment (Figure 4B). At the maximum base pH of 8.5, only ~10% of the TAN is present as dissolved NH_3, making gas extraction difficult. The acid compartment pH decreases continuously over the course of the experiment. A cation balance was again performed for the acid compartment to ensure the IEMs in the BMED stack were operating properly (Figure 4C). The cation balance shows a constant cation concentration and that NH_4^+ is

replaced with a proton in the base compartment, indicating that the CEM is working properly. The small concentration of Na^+ ion in the acid compartment is likely to have stemmed from the rinse system. However, the rate of sodium infiltration is not as significant as in the SBL configuration.

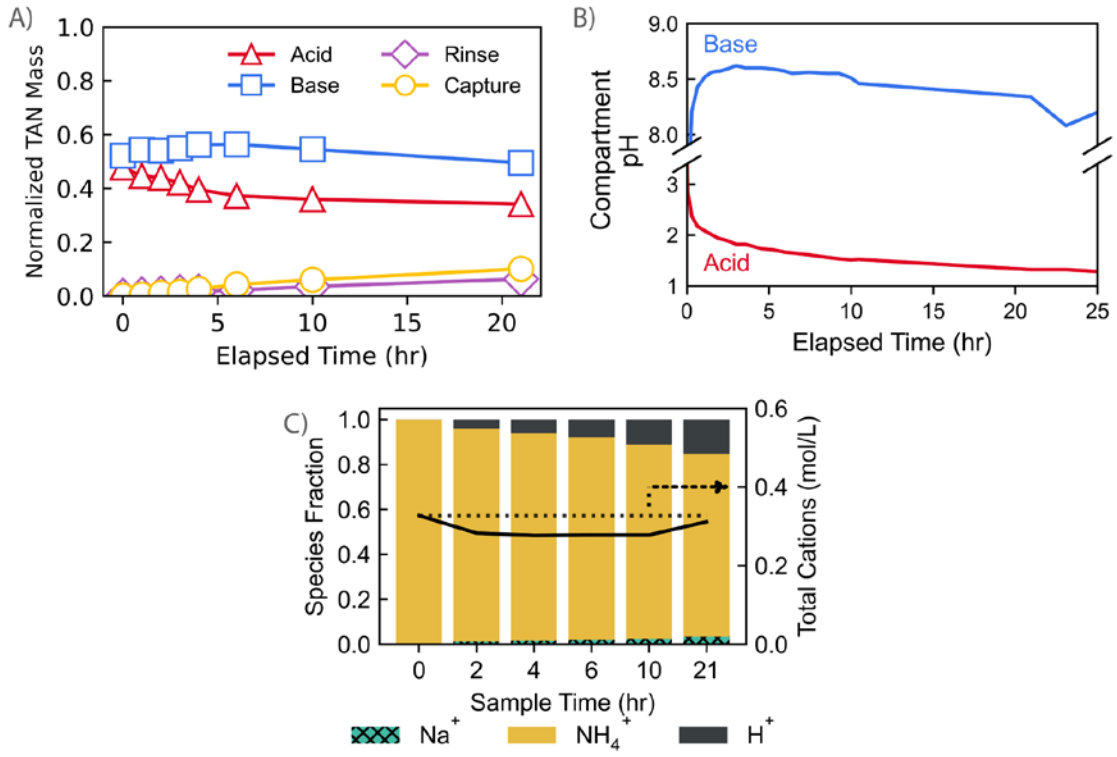

Figure 4: System performance of split-CEM configuration of BMED system. (A) TAN masses in each compartment normalized to the TAN mass in the system, showing low recovery and decreasing ammonia removal rate from acid compartment. (B) pH in acid and base compartments over the course of the experiment. (C) Cationic balance and molar fractions in acid compartment. The dotted line indicates the initial cation concentration.

It is possible that a similar phenomenon to that observed in the SBL configuration occurred: the high mobility of protons forces NH_4^+ ions back across the CEM against the electrical potential gradient. We tried running the system without gas extraction turned on to check if that would increase the pH in the base compartment, but there was no real effect. These trends were observed in multiple split-CEM configuration experiments and ammonia recovery was consistently low. Like the SBL configuration, the reverse migration of NH_4^+ in the split-CEM configuration does not allow for attaining high pH in the base compartment and therefore effective ammonia recovery was difficult.

3.3 Split-AEM Configuration

To prevent the reverse migration of NH_4^+, AEMs were employed in the split-AEM configuration where the inter-compartment movement of the protons and NH_4^+ ions is hindered. In this split-AEM configuration, the total cation concentration is expected to increase in the acid compartment as protons are generated to balance the charge of the SO_4^{2-} ions entering the acid compartment. As in the SBL and split-CEM configurations, the total cation concentration would decrease in the base compartment as NH_3 is removed from solution. The baseline operating conditions for the split-AEM configuration were: (1) an initial solution pH of 5; (2) an initial solution $(NH_4)_2SO_4$ concentration of 2000 ppm-N; (3) a 1:1 volume ratio between the acid and base compartments. All experiments were carried out at a constant 8V potential difference between electrodes. Operating conditions were varied one at a time to observe initial concentrations of 1000, 2000, and 4000 ppm-N, initial solution pH values of 2, 5, 8, and volume ratios of 1:1 and 2.3:1 between the acid and base compartments. Normalized TAN concentrations in each compartment at the end of the experiments with these different operating conditions are summarized in Figure 5A, and the numerical ammonia recovery values and experimental durations are shown in Table 3.

The base compartment TAN concentration approaches zero in all experiments, indicating that the experiments ran to near completion and the majority of extractable ammonia was recovered. In the SBL and split-CEM configurations, normalized TAN concentrations in the acid compartment were ~0.8, and ~0.4 end of the experiments, respectively. In other words, 80% and 40% of recoverable ammonia were unrecovered in the SBL configuration and split-CEM configuration, respectively. In the SBL configuration, 100% of the ammonia in the acid compartment was theoretically recoverable, but in the split-CEM configuration, only the ammonia present in the acid compartment at the start of the experiment was theoretically recoverable. In the split-AEM configuration, only the ammonia present in the base compartment at the start of the experiment was theoretically recoverable. In the split-AEM configuration, the pH of the base compartment was higher than that of the split-CEM configuration. The pH increased monotonically to ~10 by the end of the experiment (Appendix A, Figure A2). This higher pH allowed for nearly 100% of the TAN to be present as dissolved NH_3, facilitating the gas extraction.

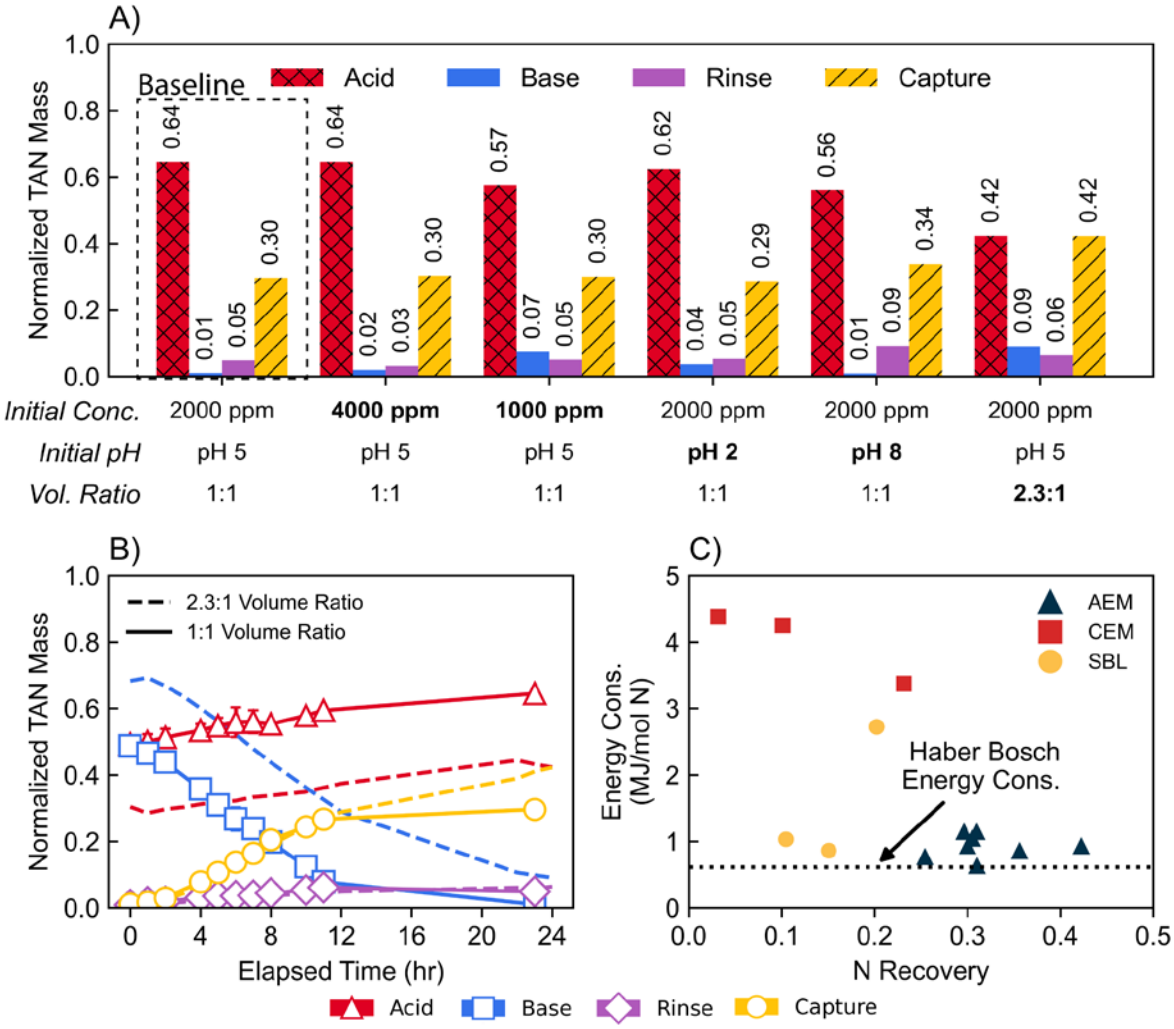

Figure 5: System performance of split-AEM configuration of BMED system. (A) TAN masses normalized to TAN mass in the system for different initial TAN concentrations, pH, and volume ratios. Values indicate the TAN concentration in each compartment at the end of the experiment. (B) TAN masses normalized to TAN mass in the system over time for different volume ratios of base and acid solutions. (C) Energy per mol of ammonia required for ammonia recovery in capture tank for different membrane configurations. The split-AEM configuration exhibits the lowest energy requirement for given ammonia recovery.

The initial normalized TAN concentration in the acid compartment is 0.5 for all experiments with a 1:1 volume ratio in Figure 5A. The increase in acid TAN concentration is due to the diffusion of neutrally charged NH_3 through the AEM from the base compartment to the acid compartment. As a result, approximately 6-15% of ammonia originating in the base compartment becomes trapped in the acid compartment. An additional 3-9% becomes trapped in the rinse compartment

due to diffusion of the neutrally charged NH_3 through the BPMs. The fraction of ammonia lost to the acid and rinse compartments at the end of each experiment is shown in Figure 5A. When the acid and base solutions were recombined together at the end of the baseline experiment, the pH of the resulting mixture was ~1.5, confirming that there was a net increase in the acid content of the solution and a net transfer of ammonia into the capture solution.

The ammonia recovery in this configuration is largely determined by the relative volume split of the MC effluent between the acid and base compartments. This is because (1) only the NH_3 that enters on the base side of the system can be extracted, and (2) the dissolved NH_3 present at higher pH is neutrally charged and is able to diffuse through IEMs and BPMs [18], [25]. While this NH_3 diffusion also occurs in the other configurations, the NH_3 that diffuses from the base to the acid compartment via the AEM becomes “trapped” in the acid compartment. In other words, once in the acid compartment, NH_3 is converted to NH_4^+ ion and prevented from crossing the AEM due to the Donnan exclusion of the membrane [19].

3.3.1 Impact of Initial Concentration

The initial $(NH_4)_2SO_4$ concentration did not have a large impact on ammonia recovery relative to the baseline conditions. The concentrations in each compartment over time are included in Appendix A, Figure A3. The normalized TAN concentrations over time almost overlap, showing that the initial concentration does not significantly impact ammonia recovery. Therefore, while recovery values are similar between different initial concentrations, absolute amounts of ammonia recovered is approximately proportional to the initial TAN concentration of the feed.

3.3.2 Impact of Initial pH

The pH 8 variation of the experiment demonstrated slightly higher ammonia recovery than either the baseline or pH 2 variations. While TAN concentration profiles over time nearly overlap for pH 5 and 8 experiments, pH 2 demonstrates a slower initial mass transfer rate (Appendix A, Figure A3). In the pH 2 experiment, the pH of the base compartment must first be increased to ~9 before ammonia recovery can take place, therefore extra time is needed to titrate the residual acid in the feed solution when starting at a low pH. Therefore, when BMED is combined with MC for ammonia recovery, the residual acid concentration in the MC effluent must be minimized to facilitate the NH_3 gas production.

3.3.3 Impact of Volume Split Ratio

In the split-AEM configuration, the feed coming from the MC is split between the acid and base compartments. In the baseline operating conditions, 50% of the flow is sent to each compartment. The flow split between compartments can be abstracted to the semi-batch experiment by adjusting the volume ratio between the acid and base solutions and the baseline case of each compartment receiving 50% of the flow is represented as a 1:1 base to acid ratio. As discussed above, the ammonia recovery from the split-AEM configuration is limited by the amount of ammonia initially in the base compartment. The highest base to acid volume ratio that could be tested with our experimental setup was ~2.3:1. The temporal changes in normalized TAN masses in the experiment are shown compared to the baseline experiment in Figure 5B. This high-volume ratio setup demonstrated the highest ammonia recovery of all the conditions tested, at ~42%. Energy Consumption and Comparative Assessment

A comparison of ammonia recoveries at the end of each experiment for the split-AEM, and the time to reach maximum recovery is shown in Table 3.

Table 3. Comparison of Recoveries from Different Split-AEM Experiments

Experimental Conditions	Total Recovery	Time to Max Recovery (hr)	Recovery from Base Compartment
Baseline (2000 pm, pH 5, 1:1 Volume Ratio)	30%	23	60%
1000-ppm Initial Concentration	30%	12	60%
4000-ppm Initial Concentration	30%	21	60%
pH 2 Initial	29%	22	58%
pH 8 Initial	34%	30 (33% at 24hrs)	68%
High Base Volume Ratio (2.3:1)	42%*	24	60%

*Highest Observed Recovery from Experiments

The energy consumption per mol of ammonia recovered by the BMED system is shown in Figure 5C. The experimental results for each BMED system configuration are plotted together against the maximum recovery achieved over the course of the experiment, along with the energy consumption of the Haber-Bosch process (~0.6 MJ/mol-N) as a reference [1]. Ammonia removal using nitrification-denitrification also consumes ~0.76 MJ/mol-N [1]. As shown in Figure 5C, the split-CEM configuration was the least energy efficient and generally achieved the lowest recovery while the split-AEM configuration was the most energy-efficient and achieved the highest recovery. The SBL configuration had comparable recovery values to split-CEM configuration, but generally similar energy consumption to the split-AEM Configuration. The relative energy consumption of the BMED process was calculated using Equation 4.

Equation 5: BMED Stack electricity consumption per mol of NH_3 Recovered

$$Relative\ Energy\ Consumption = \frac{V_{stack} \sum_{t=0}^{t=t_{\max recovery}} I_t \cdot \Delta t}{[NH_3]_{capture\ solution}^{t=t_{\max recovery}}} \quad (5)$$

The lowest energy consumption measured was 0.63 MJ/mol-N in the 4000 ppm-N experiment, using the split-AEM configuration. While we have not attempted any optimization and our system is sub-optimal, the energy consumption of the split-AEM system is comparable to the energy consumption of Haber-Bosch process for ammonia production (~0.6 MJ/mol-N) as well as that of the nitrification-denitrification process for ammonia removal (~0.76MJ/mol-N). Therefore, as MC is a spontaneous process, the integration of MC and BMED in the split-AEM configuration with further system optimization shows promise in simultaneous removal of ammonia from ammonia-rich waste streams and its valorization to ammonia gas. We note that a commercial ammonia recovery system would additionally require a compression system to produce anhydrous ammonia fertilizer that is comparable to the products currently used in agriculture and typically stored at ~10 bar [32].

Energy consumption of the system can be reduced by decreasing the spacer thickness and changing the electrode material, and operating at higher concentrations. First, a reduced spacer thickness would increase the potential gradient across the flow streams and decrease stack resistance. The spacers used in this study were 3.175 mm thick, compared to 0.2 – 1 mm in a commercial BMED stack [19], [33]. Second, different electrode materials could decrease surface potential and increase the overpotential required for any side-reactions taking place on the electrode [34][35]. Lastly, higher ammonium salt concentrations in the solutions being treated would also serve to reduce the electrical resistance of the stack. For instance, ammonia in the dilute waste stream can be greatly concentrated into an acid stream by MC, concentration factors of up to ~25, resulting in ammonia concentrations up to ~78,000 ppm has been demonstrated [36].

While such detailed design would reduce the energy consumption, some energy will be wasted in a 2-compartment BMED system. Similar to the proton flux noted in 2-compartment BMED systems using a CEM, there will be a constant flux of hydroxide ions in 2-compartment BMED systems using an AEM. When a SO_4^{2-} ion migrates out of the base compartment it is replaced with two hydroxide ions by the BPM. As these hydroxide ions are of higher mobility than other anions [31] and also capable of migrating towards the anode, transmembrane hydroxide ion flux will be a constant source of energy loss as any hydroxide ion migrating out of the base compartment will be replaced with another hydroxide.

Based on the similar ammonia recovery results from the split-AEM experiments, the system is not sensitive to changes in initial solution concentration or pH (Figure 5A). These results suggest that the split-AEM configuration can operate reliably and is not sensitive to changes in MC effluent conditions. The largest ammonia recovery from the system (i.e., combining fluids in acid, base, and rinse compartments) was observed in the high base to acid volume ratio (2.3:1) experiment, 42% compared to ~29-34% in all other scenarios. It is important to note that ammonia can only be recovered from the base compartment, not from other compartments. In the 1:1 volume ratio experiments, 50% of the total system ammonia can be recovered, and 70% in the 2.3:1 volume ratio experiment. Therefore, the ammonia recovery solely from the base compartment ($= \frac{TAN\ mass\ in\ the\ capture\ tank}{TAN\ mass\ in\ the\ base\ compartment}$) represents the recovery relative to the theoretical maximum amount of recoverable ammonia. The recovery from the base compartment was consistent between experiments, at ~60%, with the highest value of ~68% observed in the pH 8 experiment (Table 3). This somewhat low efficiency is owing to the requirement of sufficiently high pH in the base compartment necessary for NH_4^+ to NH_3 gas conversion, neutral NH_3 diffusion across the IEMs and BPMs, and accumulation of NH_3 in the rinse and acid solution. As previously described in Section 3.3 and shown in Figure 5A, for all experiments ~6-15% and ~3-9% of ammonia originating in the base compartment was trapped in the acid and rinse compartments, respectively, due to diffusion of the neutrally charged NH_3 through the IEMs and BPMs.

Higher base to acid volume ratios could further increase recovery. Still, the pH of the acid compartment would need to be maintained above the minimum, chemically tolderable, limits of the membranes. In addition, as the acid concentration in the system increases, it requires more energy for the BPM to split water to increase the acid concentration [19]. Losses to the rinse compartment can be minimized in larger BMED stacks with more repeating units. As the number of repeating units increase, the ratio of the membrane area exposed to the rinse compartments compared to the total membrane area decreases and less dissolved NH_3 will diffuse into the rinse compartments. However, diffusion losses to the acid compartment in the split-AEM system will remain constant as each repeating unit will have an interface between the acid and base compartments. Diffusion losses to the acid compartment could potentially be addressed using a 3-compartment BMED configuration, which could also address the issue of proton and hydroxide flux observed in the 2-compartment configuration. The energy loss associated with transmembrane

flux of protons or hydroxide ions could also be addressed with a 3-compartment BMED system. While 3-compartment BMED systems have higher stack resistance and design complexities, they have demonstrated lower relative energy consumption in ammonia recovery studies [21], [22].

4 Conclusion

In this work, we proposed a process that would integrate MC and BMED systems to recover ammonia from wastewater without chemical consumption. We considered three variations for a 2-compartment BMED system to interact with a MC and found that the split-AEM configuration demonstrated the highest ammonia recovery and lowest energy consumption of the systems tested. We then tested the split-AEM configuration with different operating conditions which included: (1) adjusting the inlet ammonia concentration between 1000 and 4000ppm-N, (2) adjusting the inlet solution pH between 2 and 8, and (3) adjusting the volume ratio between the base and acid compartments between 1:1 and 2.3:1. The initial concentration and pH of the feed solution had only minor impacts on ammonia recovery, allowing for a larger amount of ammonia from a MC effluent of higher NH_4^+ concentration. Increasing the base to acid volume ratio had the largest impact on ammonia recovery, ~12% higher than baseline conditions. We demonstrated that the system recovered up to ~68% of the theoretically recoverable ammonia. While the present system is sub-optimal, the energy consumption of the BMED stack was shown to be similar to the energy consumption of the Haber-Bosch ammonia production process and the nitrification-denitrification process. The energy consumption can potentially be reduced by using a higher initial ammonia concentration, decreasing spacer thickness, and using a 3-compartment BMED configuration. The ammonia recovery could be increased by further increasing the base to acid volume ratio, using a higher initial solution pH, or by implementing a 3-compartment BMED configuration. Our study demonstrates the potential of combining MC with BMED to recover ammonia from wastewater sources while minimizing chemical consumption and in an electrified method.

References

[1] H. Cruz *et al.*, “Mainstream ammonium recovery to advance sustainable urban wastewater management,” *Environ. Sci. Technol.*, vol. 53, no. 19, pp. 11066–11079, 2019.

[2] P. Kehrein, M. Van Loosdrecht, P. Osseweijer, M. Garfí, J. Dewulf, and J. Posada, “A critical review of resource recovery from municipal wastewater treatment plants-market supply potentials, technologies and bottlenecks,” *Environ. Sci. Water Res. Technol.*, vol. 6, no. 4, pp. 877–910, 2020.

[3] N. Diaz-Elsayed, N. Rezaei, T. Guo, S. Mohebbi, and Q. Zhang, “Wastewater-based resource recovery technologies across scale: A review,” *Resour. Conserv. Recycl.*, vol. 145, no. December 2018, pp. 94–112, 2019.

[4] L. Shi *et al.*, “Nutrient recovery from pig manure digestate using electrodialysis reversal: Membrane fouling and feasibility of long-term operation,” *J. Memb. Sci.*, vol. 573, no. August 2018, pp. 560–569, 2019.

[5] R. Lan, J. T. S. Irvine, and S. Tao, “Ammonia and related chemicals as potential indirect hydrogen storage materials,” *Int. J. Hydrogen Energy*, vol. 37, no. 2, pp. 1482–1494, 2012.

[6] J. G. Speight, “Industrial Inorganic Chemistry,” *Environ. Inorg. Chem. Eng.*, pp. 111–169, Jan. 2017.

[7] S. Nadarajan and S. Sukumaran, “12.3.1.2 Urea [(NH2)2CO],” in *Controlled Release Fertilizers for Sustainable Agriculture*, F. B. Lewu, T. Volova, S. Thomas, and R. K.R., Eds. Elsevier, 2021.

[8] M. Capdevila-Cortada, “Electrifying the Haber–Bosch,” *Nat. Catal.*, vol. 2, no. 12, p. 1055, 2019.

[9] R. F. Service, “Ammonia-A Renewable Fuel Made from Sun, Air, and Water-Could Power the Globe without Carbon,” *Sci. AAAS*, 2018.

[10] Q. Wei, J. M. Lucero, J. M. Crawford, J. D. Way, C. A. Wolden, and M. A. Carreon, “Ammonia separation from N2 and H2 over LTA zeolitic imidazolate framework membranes,” *J. Memb. Sci.*, vol. 623, no. October 2020, p. 119078, 2021.

[11] M. C. Garcia-González and M. B. Vanotti, “Recovery of ammonia from swine manure using gas-permeable membranes: Effect of waste strength and pH,” *Waste Manag.*, vol. 38, no. 1, pp. 455–461, 2015.

[12] P. J. Dube, M. B. Vanotti, A. A. Szogi, and M. C. García-González, “Enhancing recovery of ammonia from swine manure anaerobic digester effluent using gas-permeable membrane technology,” *Waste Manag.*, vol. 49, pp. 372–377, 2016.

[13] X. Vecino, M. Reig, O. Gibert, C. Valderrama, and J. L. Cortina, “Integration of liquid-liquid membrane contactors and electrodialysis for ammonium recovery and concentration as a liquid fertilizer,” *Chemosphere*, vol. 245, p. 125606, 2020.

[14] J. Uzkurt Kaljunen, R. A. Al-Juboori, A. Mikola, I. Righetto, and I. Konola, “Newly developed membrane contactor-based N and P recovery process: Pilot-scale field experiments and cost analysis,” *J. Clean. Prod.*, vol. 281, p. 125288, 2021.

[15] M. Darestani, V. Haigh, S. J. Couperthwaite, G. J. Millar, and L. D. Nghiem, “Hollow fibre membrane contactors for ammonia recovery: Current status and future developments,” *J. Environ. Chem. Eng.*, vol. 5, no. 2, pp. 1349–1359, 2017.

[16] USDA Economic Research Service, “Fertilizer Use and Price Dataset,” 2019. [Online]. Available: https://www.ers.usda.gov/data-products/fertilizer-use-and-price/.

[17] H. H. Taylor, “Fertilizer Use and Price Statistics 1960-93,” United States Department of

Agriculture Economic Research Service, Washington D.C., 1994.
[18] R. Pärnamäe *et al.*, “Bipolar membranes: A review on principles, latest developments, and applications,” *J. Memb. Sci.*, vol. 617, 2021.
[19] H. Strathmann, *Ion-Exchange Membrane Separation Process*, First. Amsterdam: Elsevier B.V, 2004.
[20] X. Zhang, W. Lu, H. Ren, and W. Cong, “Sulfuric acid and ammonia generation by bipolar membranes electrodialysis: Transport rate model for ion and water through anion exchange membrane,” *Chem. Biochem. Eng. Q.*, vol. 22, no. 1, pp. 1–8, 2008.
[21] N. van Linden, G. L. Bandinu, D. A. Vermaas, H. Spanjers, and J. B. van Lier, “Bipolar membrane electrodialysis for energetically competitive ammonium removal and dissolved ammonia production,” *J. Clean. Prod.*, vol. 259, p. 120788, 2020.
[22] Y. Li, S. Shi, H. Cao, X. Wu, Z. Zhao, and L. Wang, “Bipolar membrane electrodialysis for generation of hydrochloric acid and ammonia from simulated ammonium chloride wastewater,” *Water Res.*, vol. 89, pp. 201–209, 2016.
[23] M. A. B. Ali, M. Rakib, S. Laborie, P. Viers, and G. Durand, “Coupling of bipolar membrane electrodialysis and ammonia stripping for direct treatment of wastewaters containing ammonium nitrate,” *J. Memb. Sci.*, vol. 244, no. 1–2, pp. 89–96, 2004.
[24] C. Huang, T. Xu, Y. Zhang, Y. Xue, and G. Chen, “Application of electrodialysis to the production of organic acids: State-of-the-art and recent developments,” *J. Memb. Sci.*, vol. 288, no. 1–2, pp. 1–12, 2007.
[25] J. S. Jaime-Ferrer, E. Couallier, P. Viers, and M. Rakib, “Two-compartment bipolar membrane electrodialysis for splitting of sodium formate into formic acid and sodium hydroxide: Modelling,” *J. Memb. Sci.*, vol. 328, no. 1–2, pp. 75–80, 2009.
[26] H. Liu and J. Wang, “Separation of ammonia from radioactive wastewater by hydrophobic membrane contactor,” *Prog. Nucl. Energy*, vol. 86, pp. 97–102, 2016.
[27] X. Vecino, M. Reig, B. Bhushan, O. Gibert, C. Valderrama, and J. L. Cortina, “Liquid fertilizer production by ammonia recovery from treated ammonia-rich regenerated streams using liquid-liquid membrane contactors,” *Chem. Eng. J.*, vol. 360, no. September 2018, pp. 890–899, 2019.
[28] L. Yu, J. Su, and J. Wang, “Bipolar membrane-based process for the recycle of p-toluenesulfonic acid in D-(-)-p-hydroxyphenylglycine production,” *Desalination*, vol. 177, no. 1–3, pp. 209–215, 2005.
[29] J. H. Choi, S. H. Kim, and S. H. Moon, “Recovery of lactic acid from sodium lactate by ion substitution using ion-exchange membrane,” *Sep. Purif. Technol.*, vol. 28, no. 1, pp. 69–79, 2002.
[30] C. Lei *et al.*, “Comparative study on the production of gluconic acid by electrodialysis and bipolar membrane electrodialysis: Effects of cell configurations,” *J. Memb. Sci.*, vol. 608, no. January, p. 118192, 2020.
[31] CRC Press, *CRC Handbook of Chemistry and Physics*, 102nd ed. Taylor & Francis Group, 2021.
[32] H. Pasman, “Industrial Processing Systems, Their Products and Hazards,” *Risk Anal. Control Ind. Process. - Gas, Oil Chem.*, pp. 1–31, Jan. 2015.
[33] K. M. Chehayeb, D. M. Farhat, K. G. Nayar, and J. H. Lienhard, “Optimal design and operation of electrodialysis for brackish-water desalination and for high-salinity brine concentration,” *Desalination*, vol. 420, no. July, pp. 167–182, 2017.
[34] S. Shin, K. Kim, and J. Choi, “Fabrication of ruthenium-doped TiO2 electrodes by one-step

anodization for electrolysis applications," *Electrochem. commun.*, vol. 36, pp. 88–91, 2013.
[35] C. Comninellis and G. Chen, Eds., *Electrochemistry for the Environment*. Springer, 2010.
[36] X. Vecino, M. Reig, B. Bhushan, O. Gibert, C. Valderrama, and J. L. Cortina, "Liquid fertilizer production by ammonia recovery from treated ammonia-rich regenerated streams using liquid-liquid membrane contactors," *Chem. Eng. J.*, vol. 360, no. November 2018, pp. 890–899, 2019.

Appendices

Appendix A: Supplemental Information

Experimental Setup Details

Acid and rinse bottles are borosilicate glass with a custom-made cap and fittings to ensure proper sealing around the tubing entering and exiting the bottle. The base and capture tanks are made out of Sch 80 PVC, with custom flange lids sealed with Viton® gaskets. Tubing is ¼" OD FEP, with PVDF push to connect fittings. The valves used for base tank and stack isolation are either PVC or PVDF. The BMED stack is made of 1" PVC faceplates, with 1/8" PVDF spacers, and 0.8mm Viton® gaskets. 3-D printed turbulence promoters were added in each spacer to maintain proper spacing of the flow compartments when under pressure. The 3-D printing material is "Accura Xtreme White 200" and the parts were made by Forge Labs in Burnaby, BC. There are three repeating units in the BMED stack. The active area for each membrane is 25cm^2 (5cm x 5cm).

Acid, base, and rinse solutions are circulated through the stack at ~1LPM using *Masterflex Console Gear Pumps* and *Micropump L21830 A-Mount Cavity Style Pump Head*s (Items *RK-75211-12* and *RK-07001-40* from Cole-Parmer). Tubing was run so that fluid flowed from the bottom-up to avoid air pockets inside the stack. The system voltage was controlled and the current measured by a Bio-Logic SP-200 Potentiostat. pH measurements for the acid and base compartment were measured in-line using an *Omega-PHH-37* and *Oakton pH 5+* pH meter. The circulating pressure of each fluid was measured downstream of the pump and upstream of the BMED stack. The headspace pressure was monitored in the base, rinse, and capture tanks, and there was no headspace in the acid tank. Without the addition of the pressure relief valve, the rinse bottle would need to be burped approximately once every 45 minutes or else rinse solution would enter the acid and base compartments. This was indicated by a sudden increase in system current. A photo of the experimental setup is shown in Figure A1.

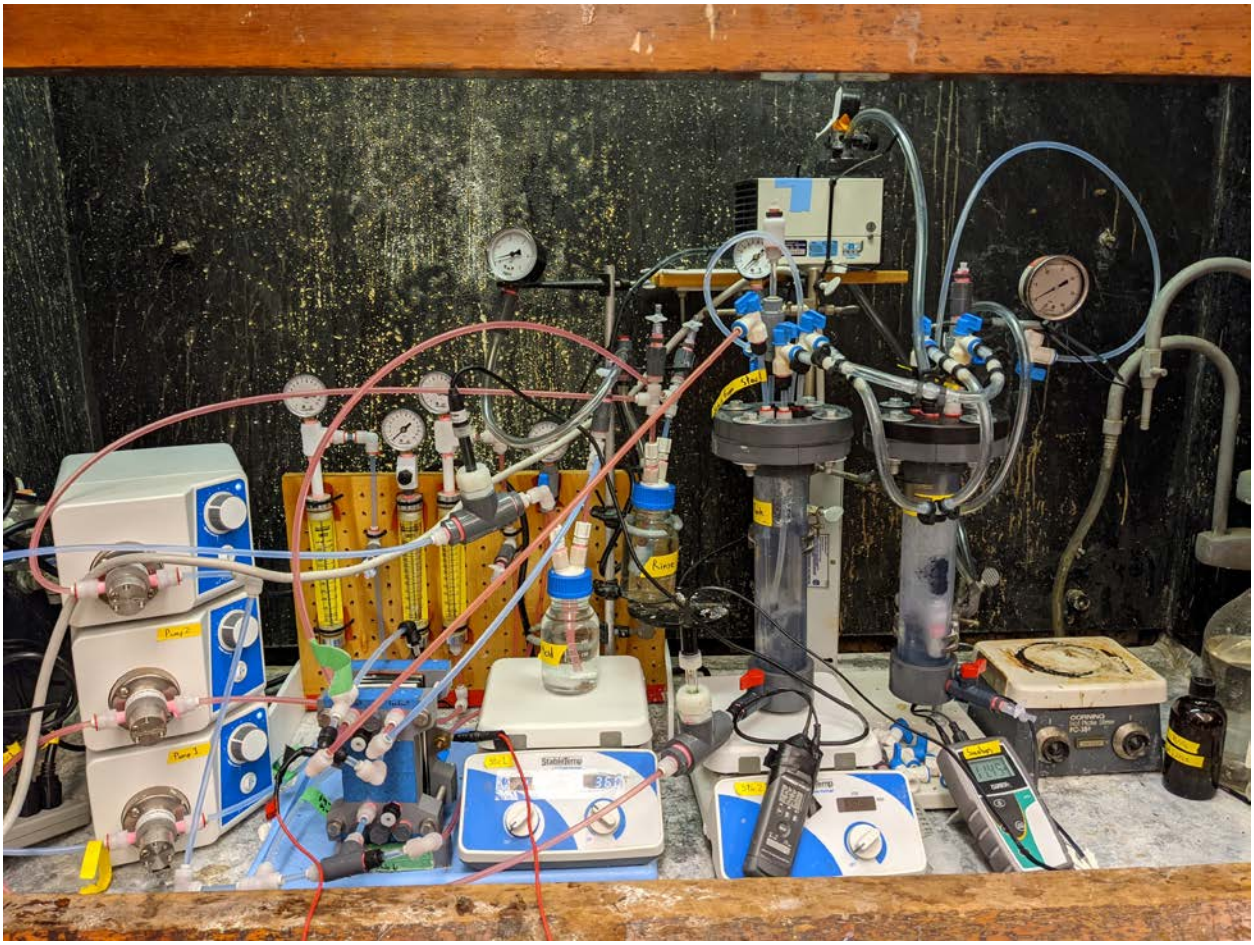

Figure A1: Experimental setup inside fume hood

Troubleshooting SBL and Split-CEM Configurations

The SBL and split-CEM configurations did not demonstrate high ammonia recovery or As these results were unexpected, it was important to determine whether there was an issue with the system setup. The system was troubleshooted by: (1) confirming potential difference and current with an external multi-meter; (2) checking the stack for leaks under pressure; (3) disassembling the stack to check for gasket leaks; (4) inspecting the membranes for damage; and (5) flowing solution through one compartment at a time to check for leaks between compartments. However, it was possible that fluid from the base compartment was leaking into the acid compartment, or that the CEM was somehow ineffective. However, the volume of the base tank remained constant over the course of the experiment. To confirm that the ion-exchange membranes were functioning properly, a cation balance was performed on the acid compartment. If the BMED stack is operating correctly,

the total concentration of cations in the acid compartment will be constant throughout the experiment.

If fluid from the base compartment was leaking into the acid compartment, or if anions such as SO_4^{2-} and hydroxide were able to cross the CEM, we would expect to see an increase in the acid cation concentration. Given that we do not see this in any of the SBL experiments, we can assume that the CEMs are working correctly.

Additional Split-AEM Configuration Data

Figure A2 shows the pH in acid and base compartments in split-AEM experiments at different initial solution TAN concentration and pH. Figure S2B shows the lag in base compartment pH for the pH 2 experiment. The pH 2 experiment normalized TAN concentration, Figure S3B, demonstrates slower mass transfer to the capture solution compared to the pH 5 and 8 experiments.

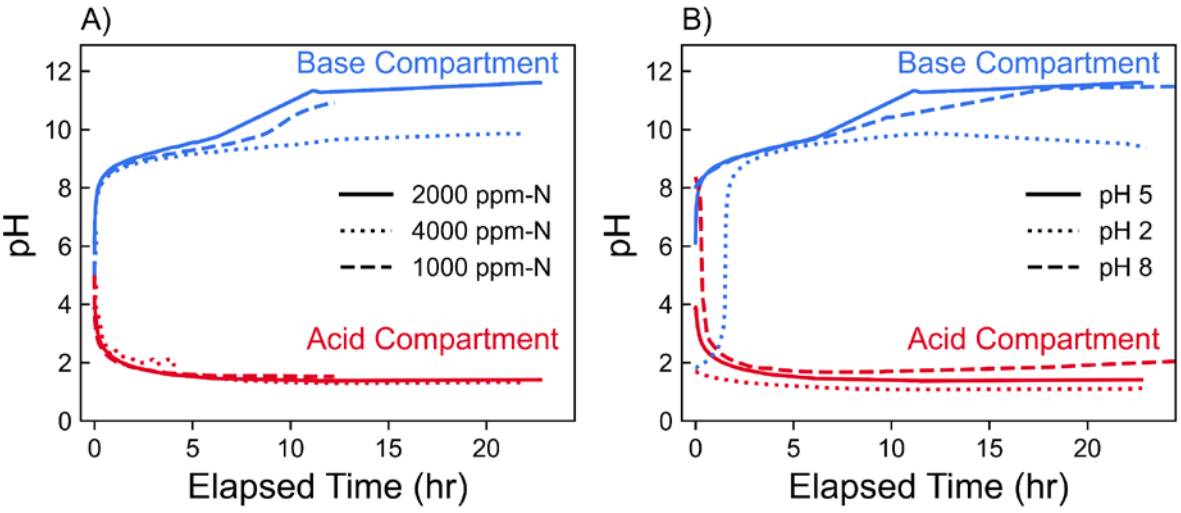

Figure A2: Solution pH in acid and base compartments for split-AEM experiments with: A) Different initial solution TAN Concentrations, B) Different initial solution pH

Figure A3 shows the normalized TAN concentrations for experiments performed with the split-AEM configuration. Concentrations at the end of the experiment are shown in Figure 5.

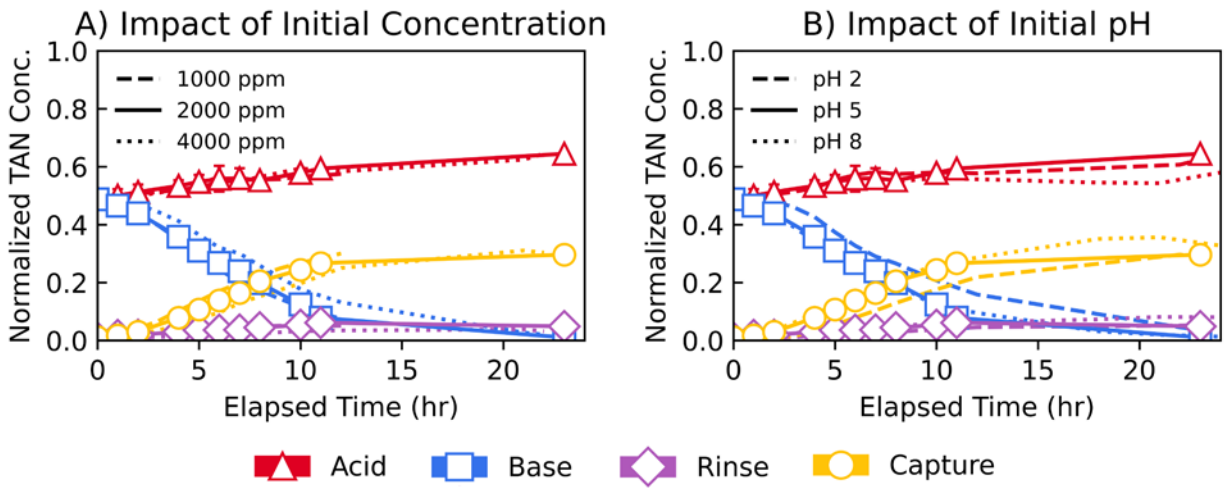

Figure A3: Normalized TAN concentrations over time in the split-AEM configuration experiments comparing A) Different initial solution ammonia concentrations, B) Different initial solution pH

Appendix B – Mechanical Drawings

Mechanical drawings for the custom parts machined and 3-D printed for this project are included in this appendix.

Drawing	Page	Name	Type	Material	Manufacturing Method
1	33	End Plate	Part	PVC	Waterjet
2	34	Electrode	Part	SS 316	Waterjet
3	35	Gasket	Part	Viton®	Waterjet
4	36	Spacers	Part	PVDF	Waterjet
5	37	Membrane	Part	Membrane	Cut by Hand
6	38	Vacuum Pressure Tank	Assembly	PVC Pipe Fittings	Hand Tools/Power Tools
7	39	Vacuum Pressure Tank Lid Hole Pattern	Part	2” Sch 80 PVC Blind Flange	Hand Tools, Power Tools
8	40	Calpac Cap Custom Fitting	Part/Assembly	Accura Extreme White	3D Printing-Forge Labs-Stereolithography
9	41	Woven Flow Spacer	Part	Accura 25	3D Printing-Forge Labs-Stereolithography
10	42	Anode Assembly	Assembly	-	-
11	43	Cathode Assembly	Assembly	-	-
12	44	Repeating Unit -2 Cell Configuration	Assembly	-	-

Stack End Plates

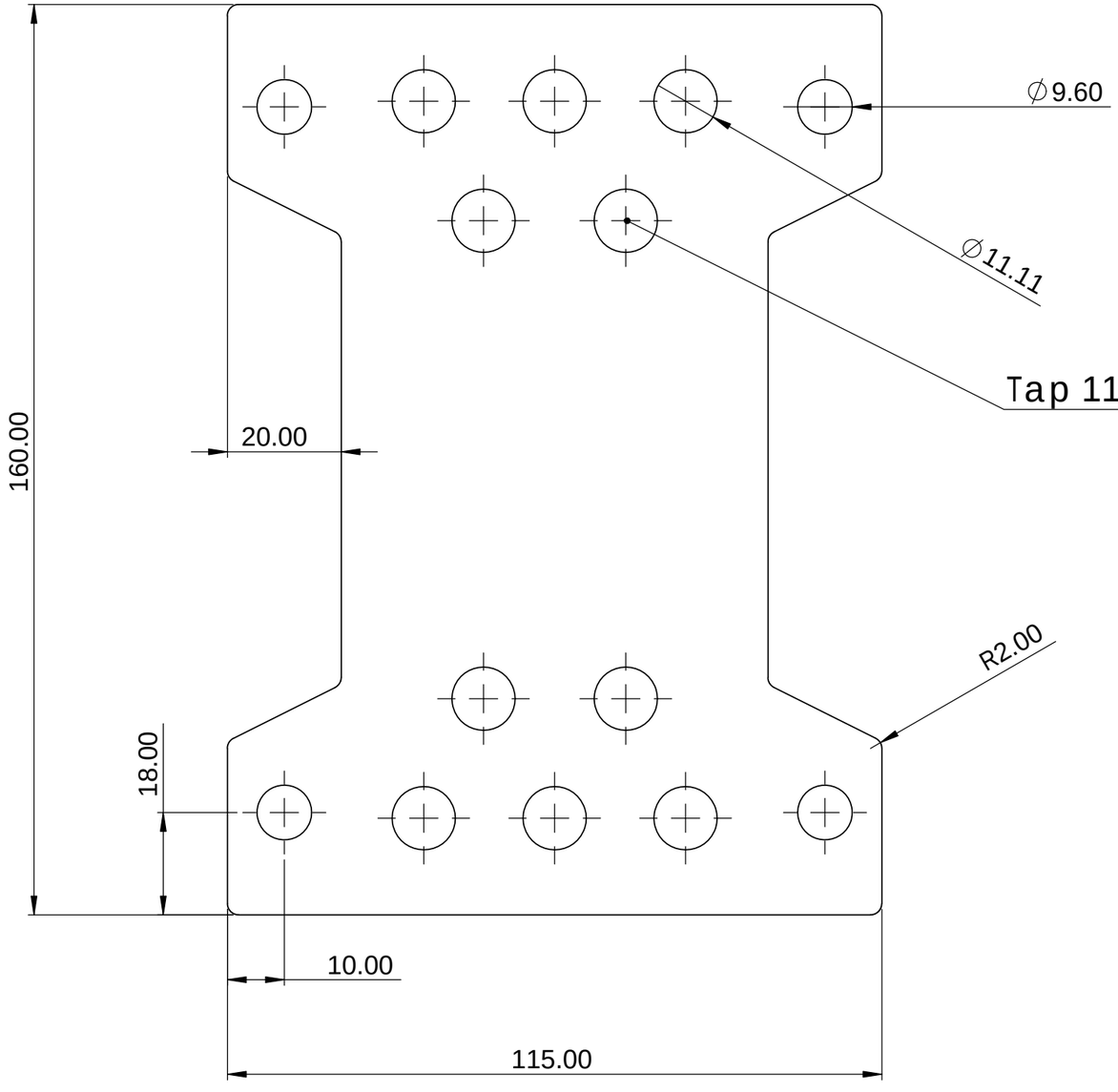

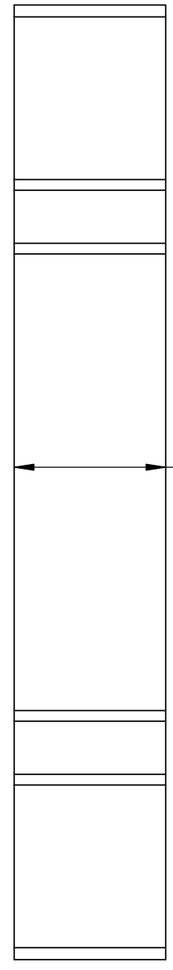

Project: Electrodialysis / Bipolar-membrane Electrodialysis Stack		
Title: ED / BMED Stack Components		
Subtitle: Stack end plate		
Drawn by: David Saabas	**Date:** Jan 13 2021	
Units: All dimensions in mm	Appendix B Drawing 1 of 12	
Sheet Size: 11" x 17"	**Sheet Scale:** 1:1	**Revision:** 1

Electrode

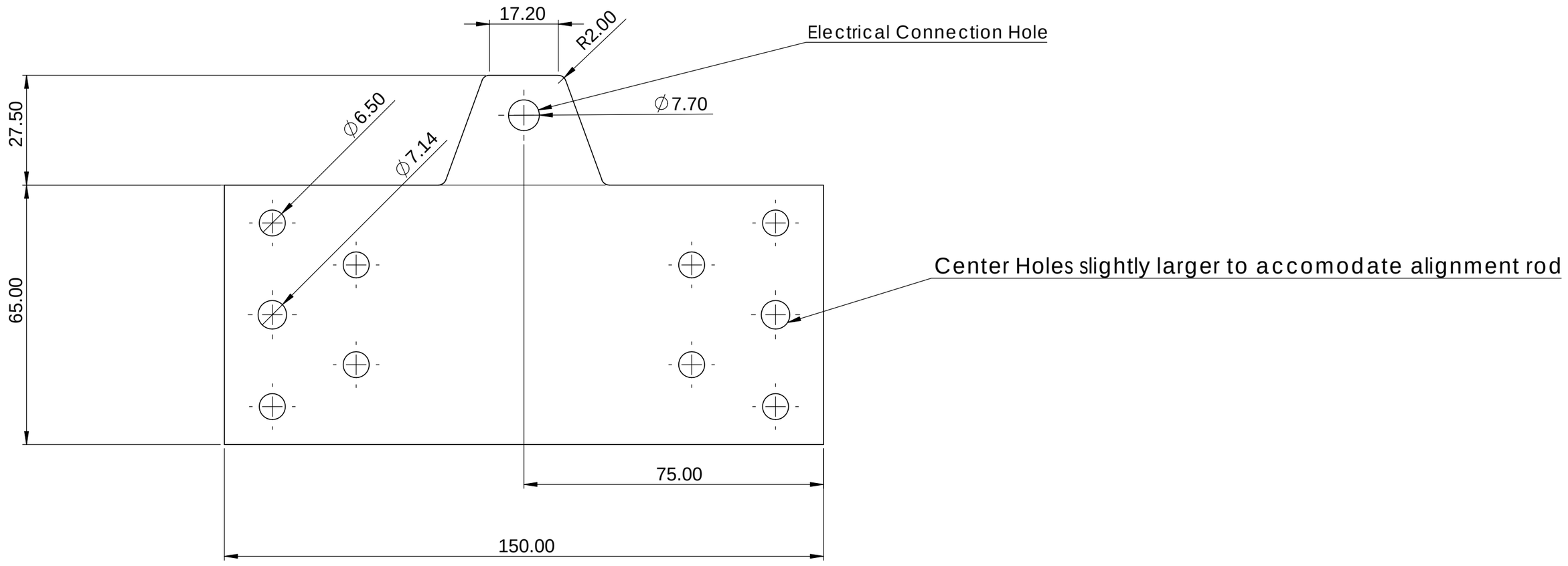

Electrode is cut out of either 1/8" SS316 or 1/4" Graphite

Project: Electrodialysis / Bipolar-membrane Electrodialysis Stack		
Title: ED / BMED Stack Components		
Subtitle: Electrode		
Drawn by: David Saabas	**Date:** Jan 13 2021	
Units: All dimensions in mm	Appendix B Drawing 2 of 12	
Sheet Size: 11" x 17"	**Sheet Scale:** 1:1	**Revision:** 1

Open Gasket

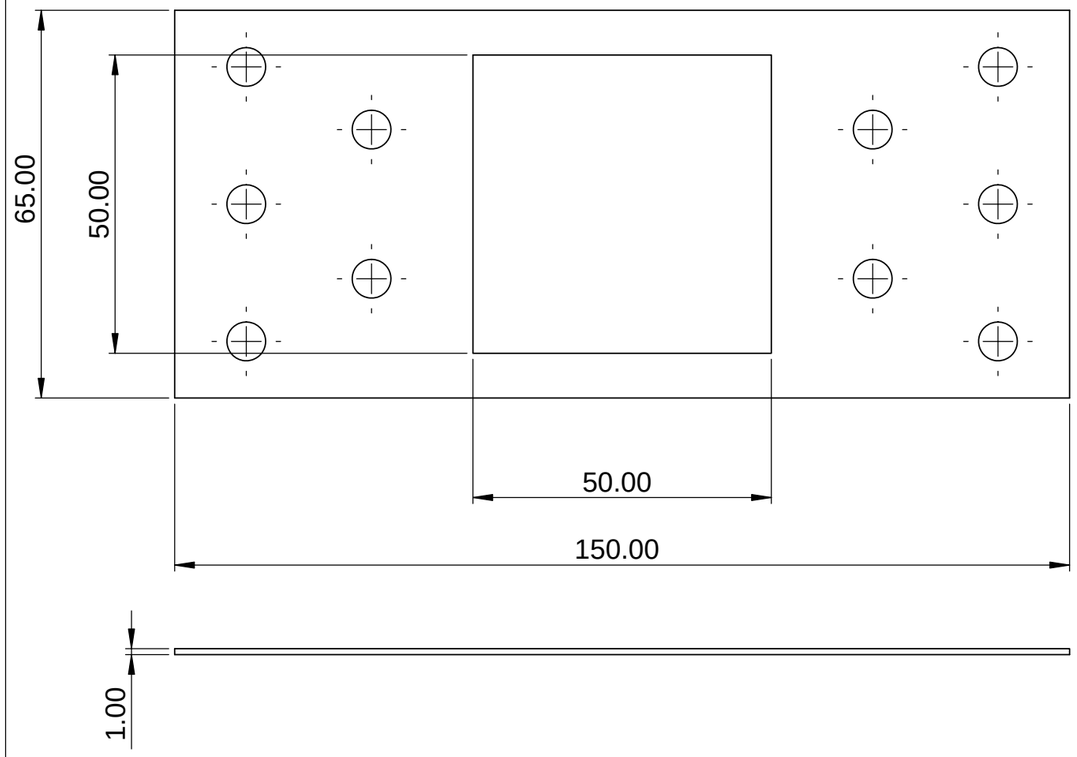

Full Gasket

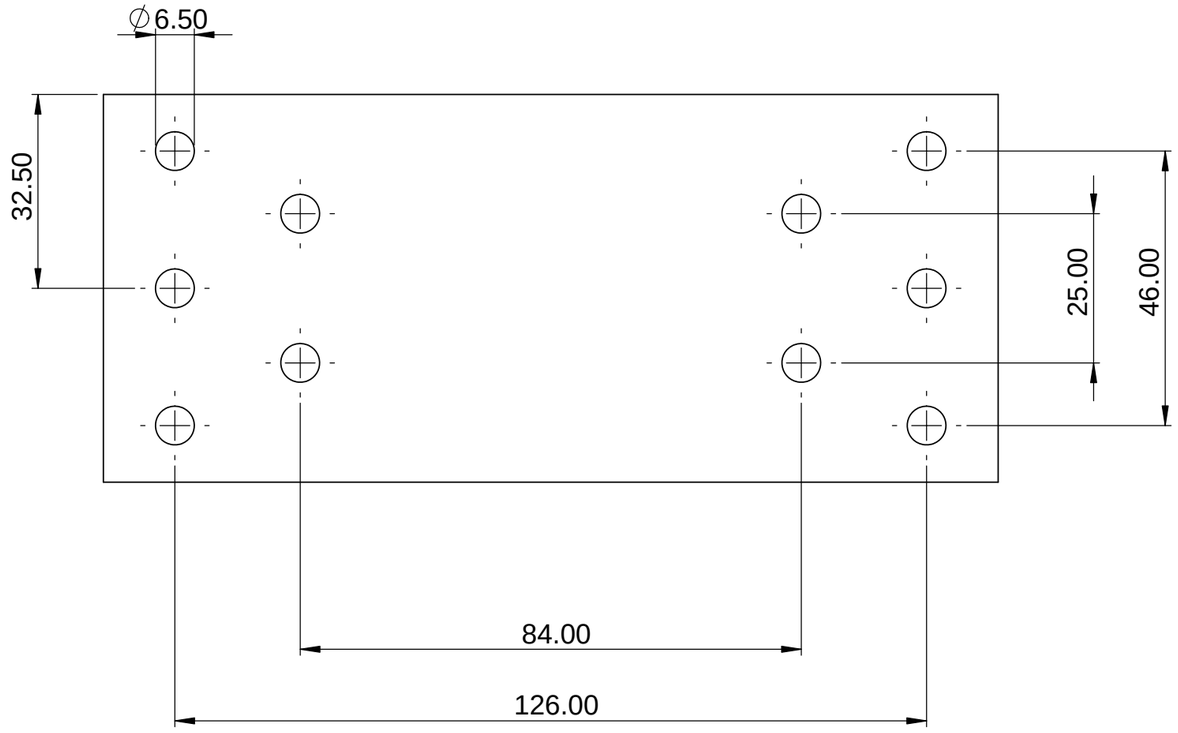

Project: Electrodialysis / Bipolar-membrane Electrodialysis Stack		
Title: ED / BMED Stack Components		
Subtitle: Standard Open and Full Gasket - 1mm Sllicone		
Drawn by: David Saabas	**Date:** Jan 13 2021	
Units: All dimensions in mm	Appendix B Drawing 3 of 12	
Sheet Size: 11" x 17"	**Sheet Scale:** 1:1	**Revision:** 1

Raw / Product Spacer

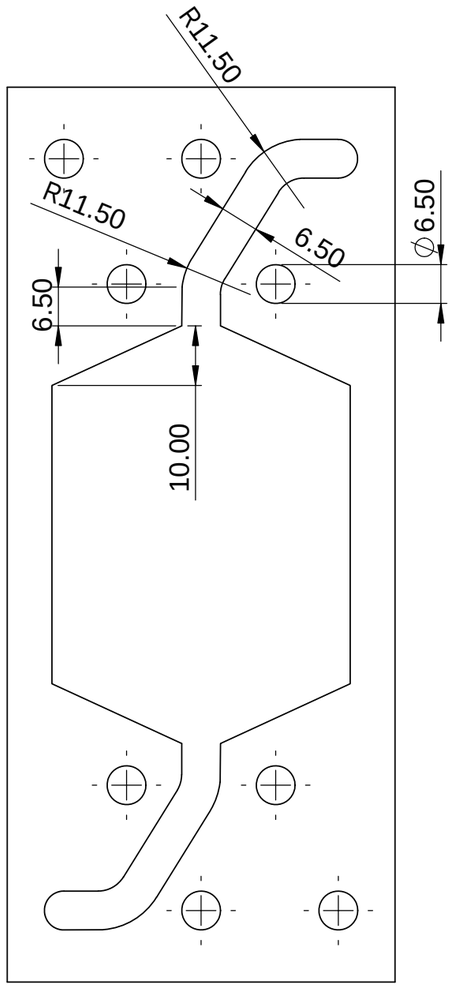

Center Flow Spacer

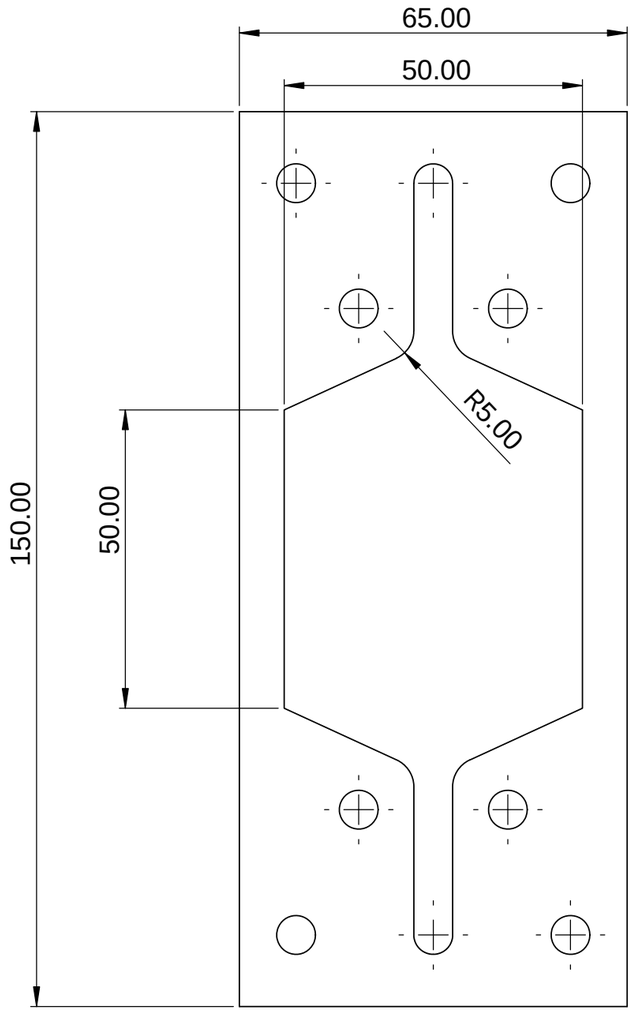

Rinse Spacer

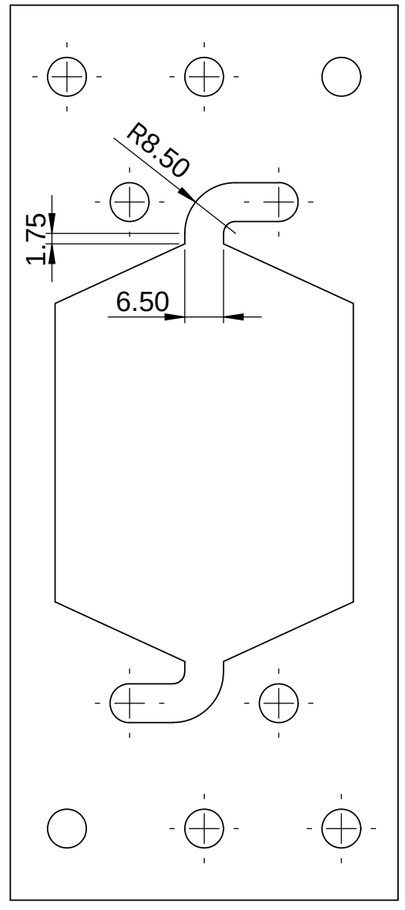

Project: Electrodialysis / Bipolar-membrane Electrodialysis Stack		
Title: ED / BMED Stack Components		
Subtitle: Spacer Types: Raw/Product, Center Flow, Rinse		
Drawn by: David Saabas	**Date:** Jan 13 2021	
Units: All dimensions in mm	Appendix B Drawing 4 of 12	
Sheet Size: 11" x 17"	**Sheet Scale:** 1:1	**Revision:** 1

Membrane Hole Pattern

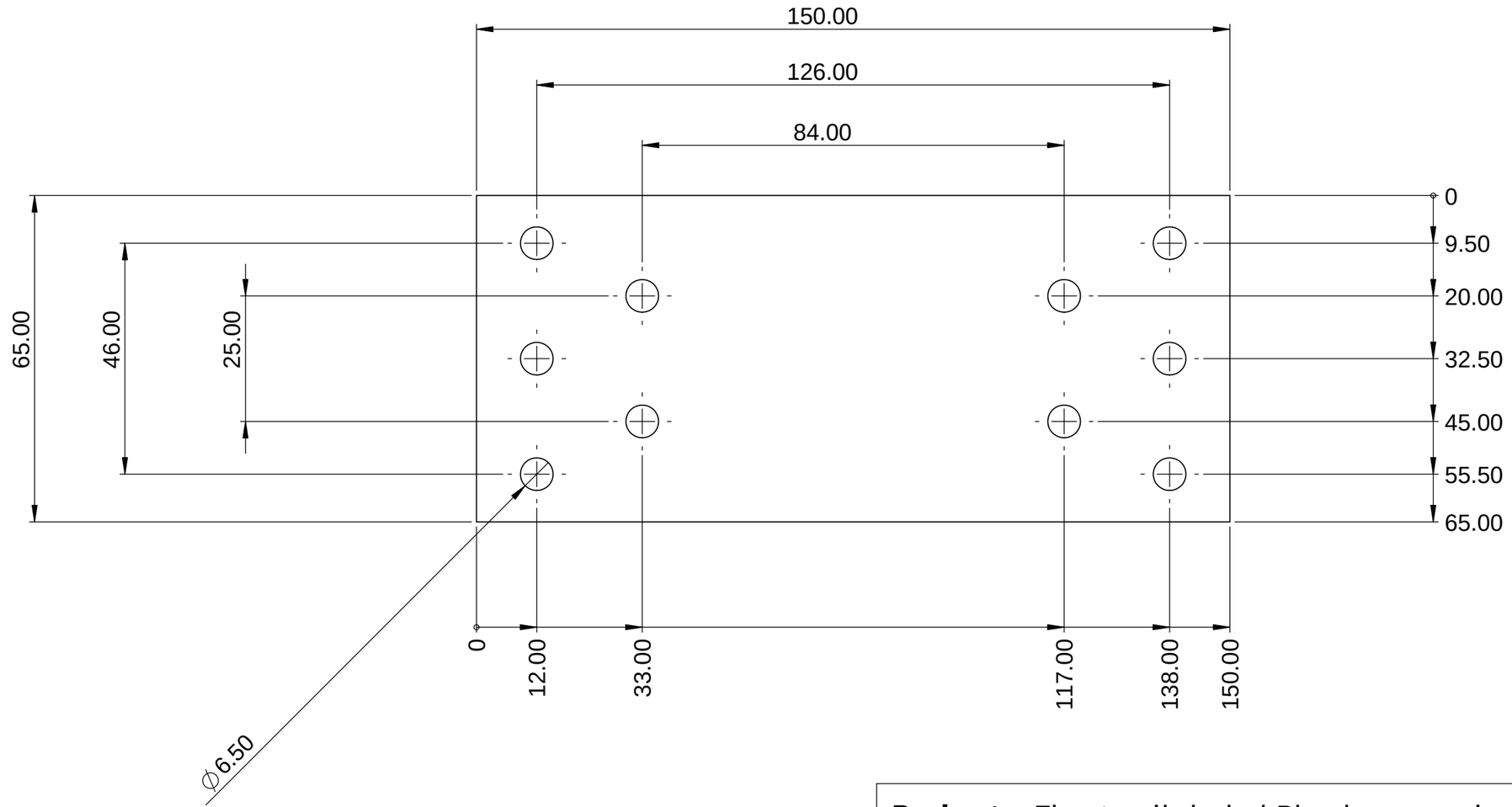

Project: Electrodialysis / Bipolar-membrane Electrodialysis Stack		
Title: ED / BMED Stack Components		
Subtitle: Membrane Hole Cutting Pattern - to scale		
Drawn by: David Saabas	**Date:** Jan 13 2021	
Units: All dimensions in mm	Appendix B Drawing 5 of 12	
Sheet Size: 11" x 17"	**Sheet Scale:** 1:1	**Revision:** 1

Vacuum / Pressure Tank

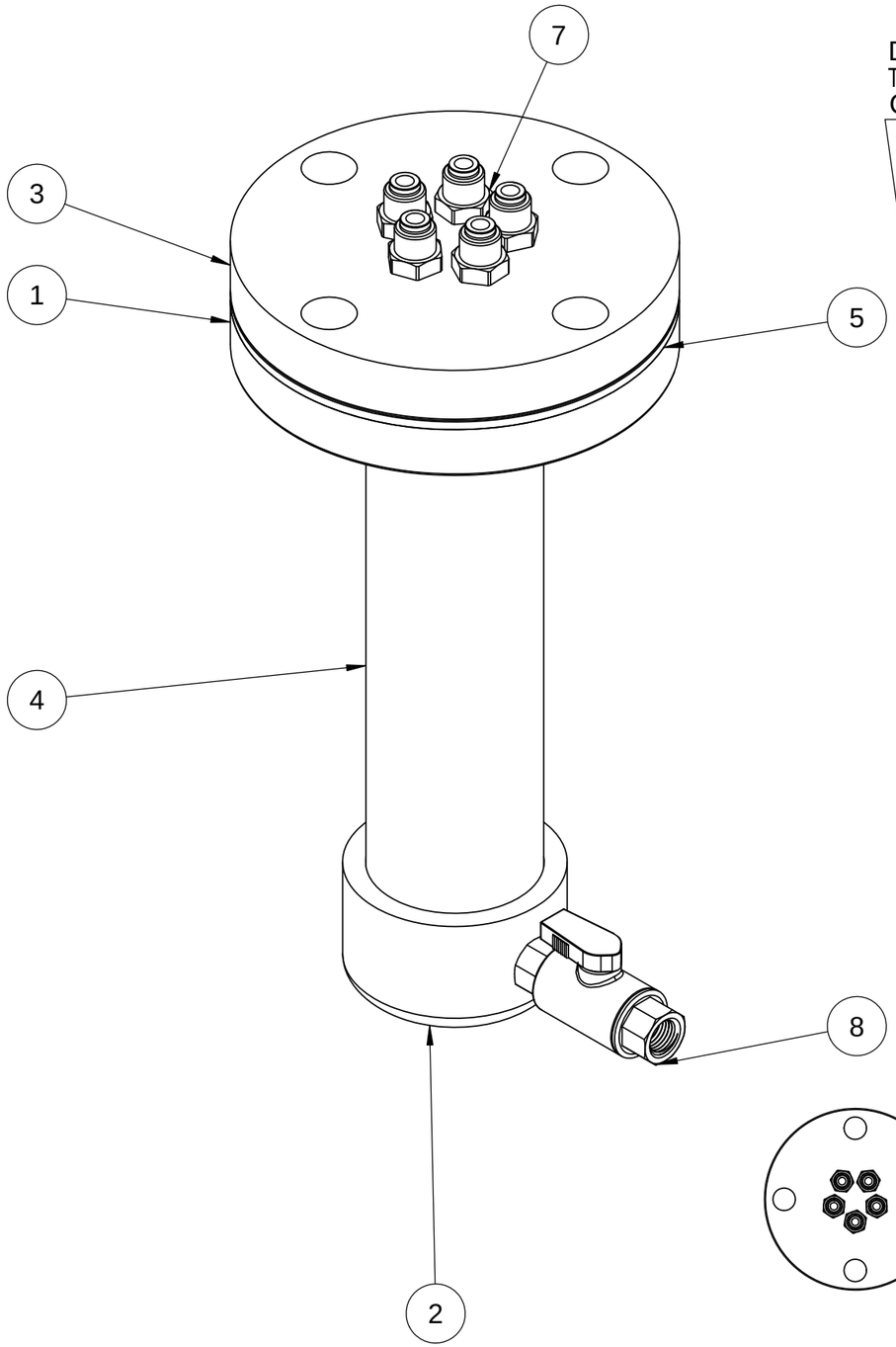

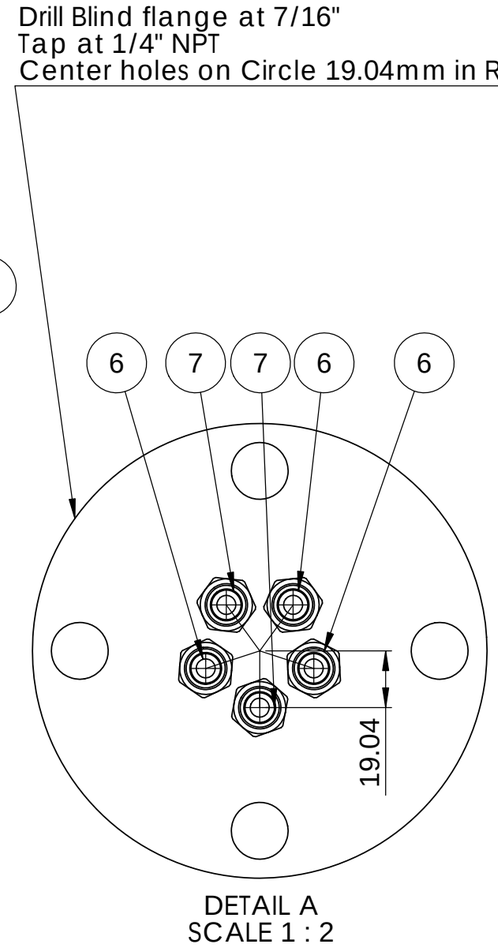

ITEM NO.	PART NUMBER	QTY.
1	2" Sch 80 PVC Blind Flange	1
2	2" Sch 80 PVC Cap	1
3	Modified 2" Sch 80 PVC Blind Flange	1
4	2" Sch 80 Clear PVC Pipe	1
5	1/16" Thick 2" Silicone Flange Gasket	1
6	0.25IN PTC by 0.25IN NPTF PVDF Fitting	3
7	0.25IN PTC by 0.25IN NPTF PVDF Fitting	2
8	45975K260_MINIATURE PVC HIGH-FLOW BALL VALVE	1

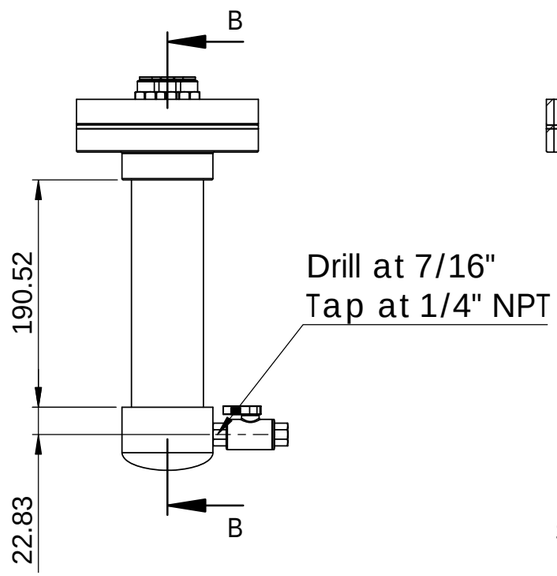

Project: Vacuum / Pressure Tank for BMED Process		
Title: ED / BMED Stack Components		
Subtitle: Vacuum / Pressure Tank		
Drawn by: David Saabas	**Date:** Jan 13 2021	
Units: All dimensions in mm	Appendix B Drawing 6 of 12	
Sheet Size: 11" x 17"	**Sheet Scale:** 1:1	**Revision:** 1

Blind Flange Lid - Cutting Template

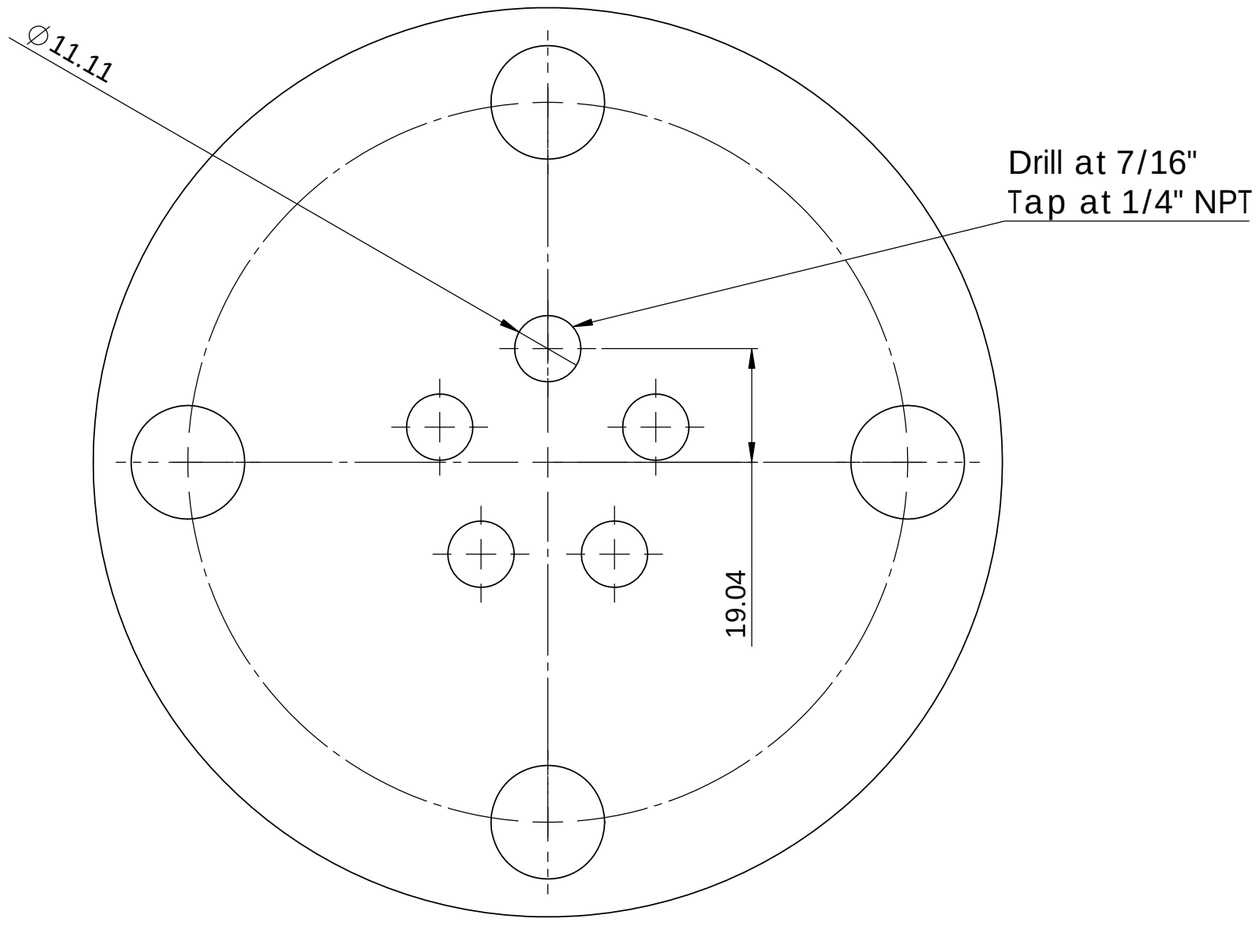

Project: Electrodialysis / Bipolar-membrane Electrodialysis Stack		
Title: ED / BMED Stack Components		
Subtitle: Lid for Vacuum Tank - Cutting Tank		
Drawn by: David Saabas	**Date:** Jan 13 2021	
Units: All dimensions in mm	Appendix B Drawing 7 of 12	
Sheet Size: 11" x 17"	**Sheet Scale:** 1:1	**Revision:** 1

Calpac Cap Special Fitting

ITEM NO.	PART NUMBER	QTY.
1	Calpac CapTop	1
2	Calpac Cap O Ring	2
3	Calpac Cap Special Fitting	2
4	5016K422	2

This part was 3-D Printed

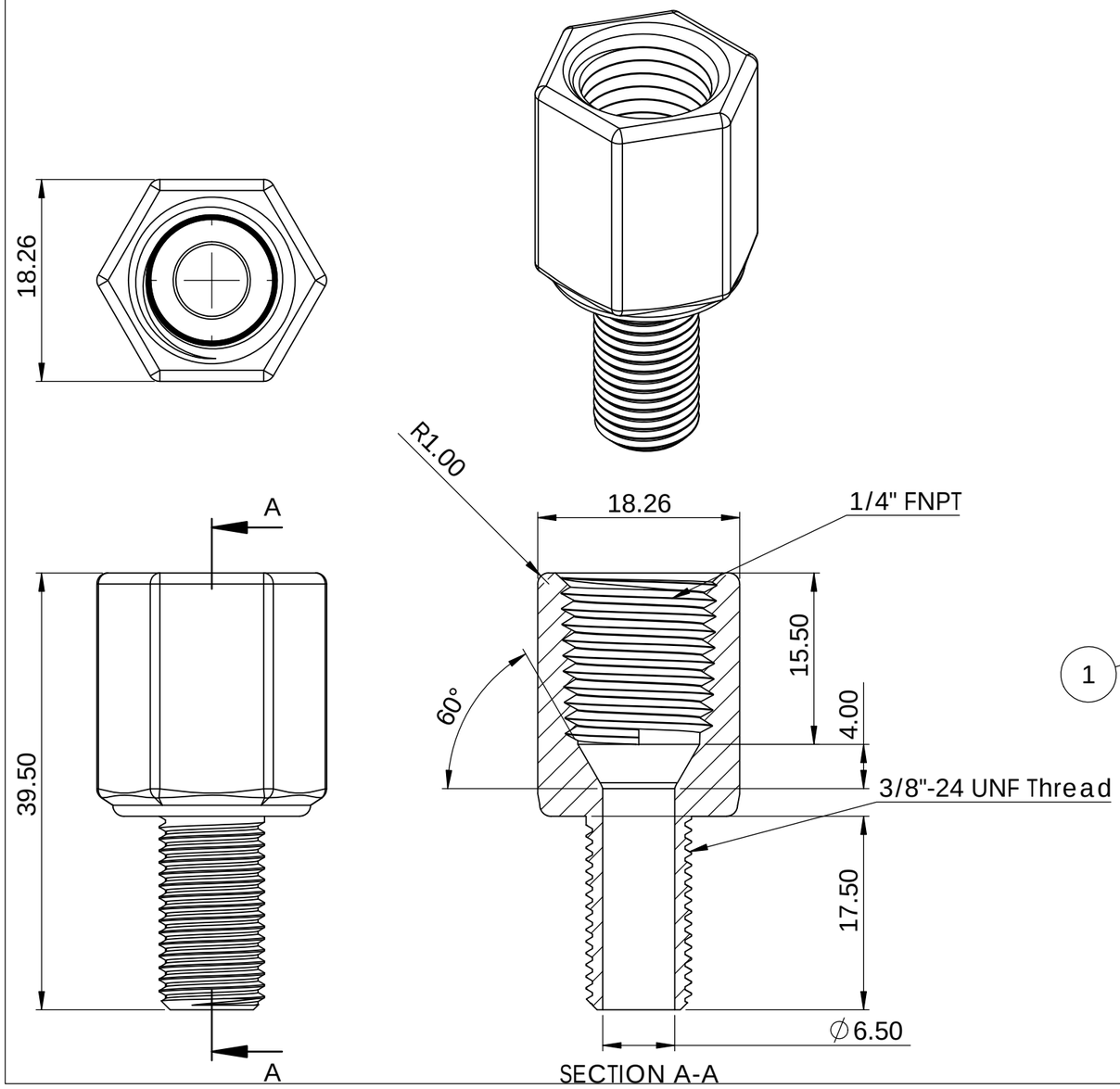

Sealing Calpac Cap Assembly

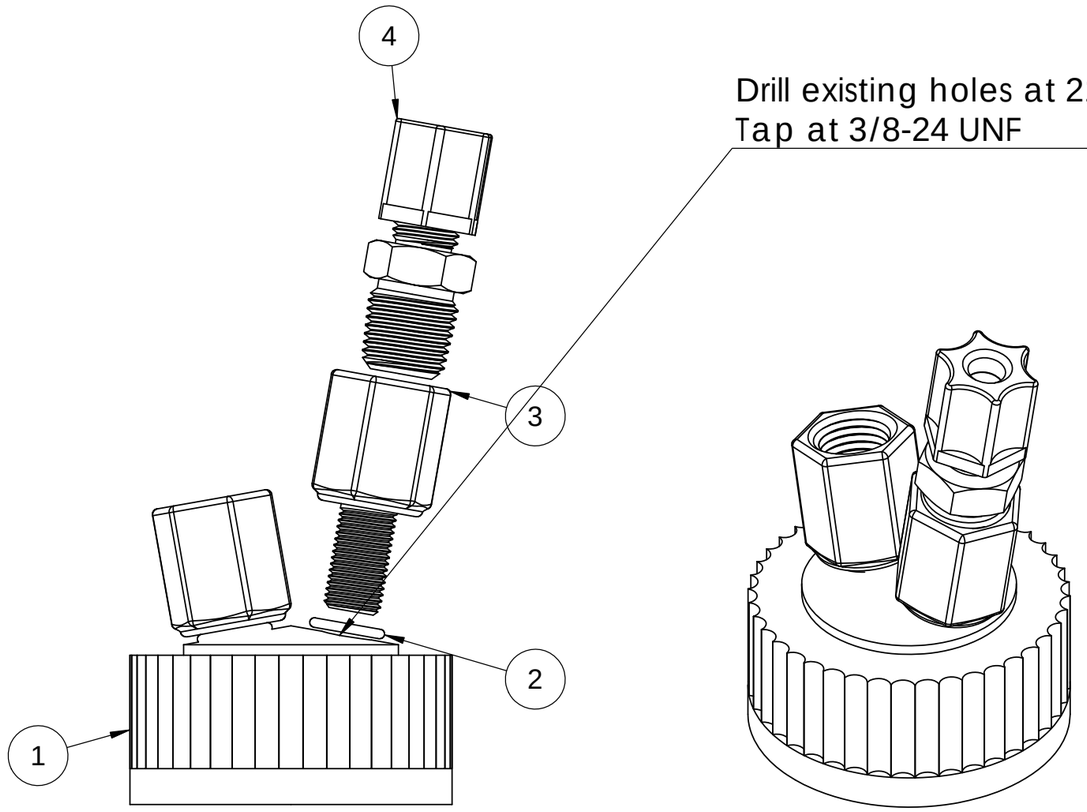

Project: Electrodialysis / Bipolar-membrane Process Equipment		
Title: Sealing Cap for Calpac Bottles		
Subtitle: Assembly and Custom Fitting		
Drawn by: David Saabas	**Date:** Jan 13 2021	
Units: All dimensions in mm	Appendix B Drawing 8 of 12	
Sheet Size: 11" x 17"	**Sheet Scale:** 2:1 , 1:1	**Revision:** 1

Turbulence Promoter - 3mm thick

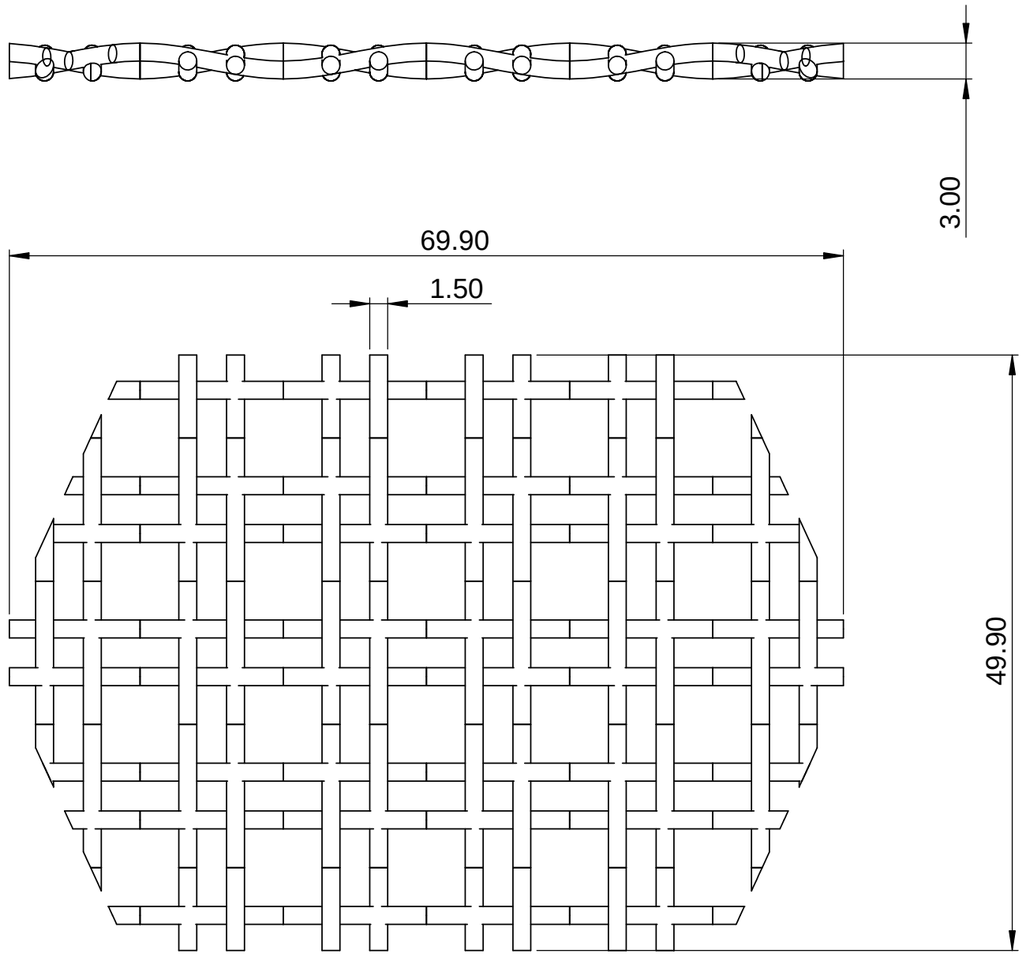

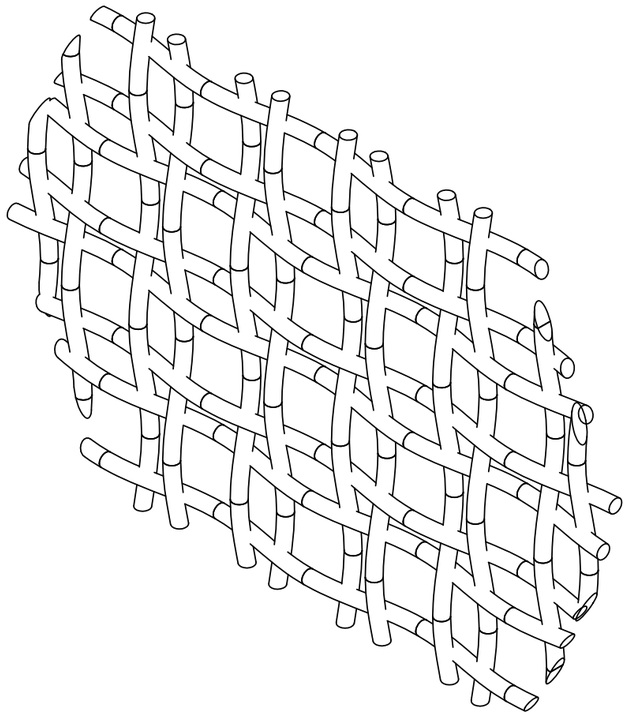

Spacer is composed of partially overlapping strands and is 3-D Printed

Fits into the 1/8" flow cells, for 0.8mm flow cells spacer is cut out of pre-fabricated plastic mesh by hand

Project: Electrodialysis / Bipolar-membrane Electrodialysis Stack		
Title: ED / BMED Stack Components		
Subtitle: 3mm Thick 3-D printed turbulence promoter		
Drawn by: David Saabas	**Date:** Jan 13 2021	
Units: All dimensions in mm	Appendix B Drawing 9 of 12	
Sheet Size: 11" x 17"	**Sheet Scale:** 1:1	**Revision:** 1

Anode Assembly

ITEM NO.	PART NUMBER	QTY.
1	Full Gasket	1
2	BMED End Plate	1
3	BMED Full Side Electrode	1
4	Open Gasket	1
5	Rinse	1
6	Woven Flow Spacer	1

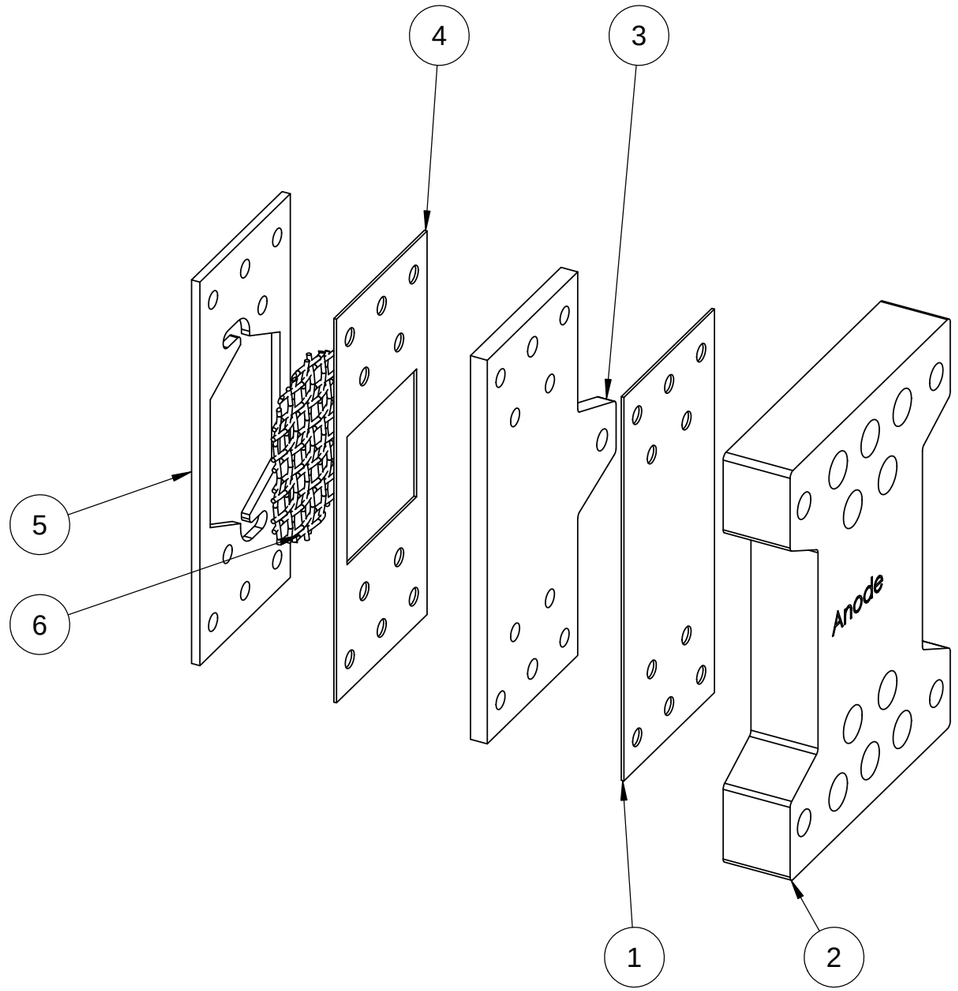

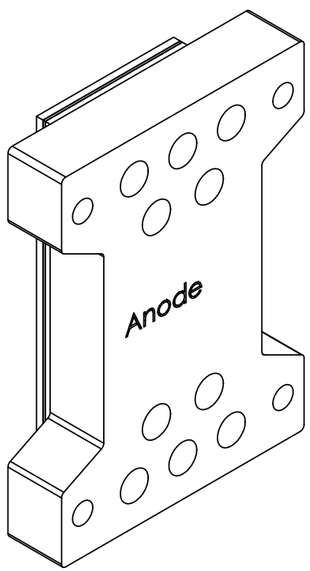

Project: Electrodialysis / Bipolar-membrane Electrodialysis Stack		
Title: ED / BMED Stack Components		
Subtitle: BMED Anode Assembly		
Drawn by: David Saabas	**Date:** Jan 13 2021	
Units: All dimensions in mm	Appendix B Drawing 10 of 12	
Sheet Size: 11" x 17"	**Sheet Scale:** 1:2	**Revision:** 1

Cathode Assembly

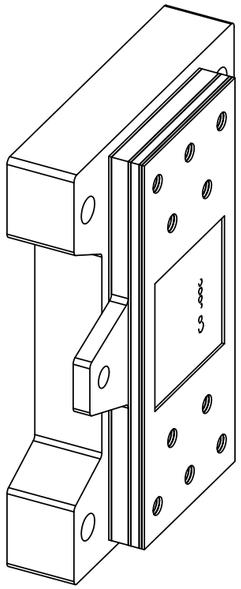

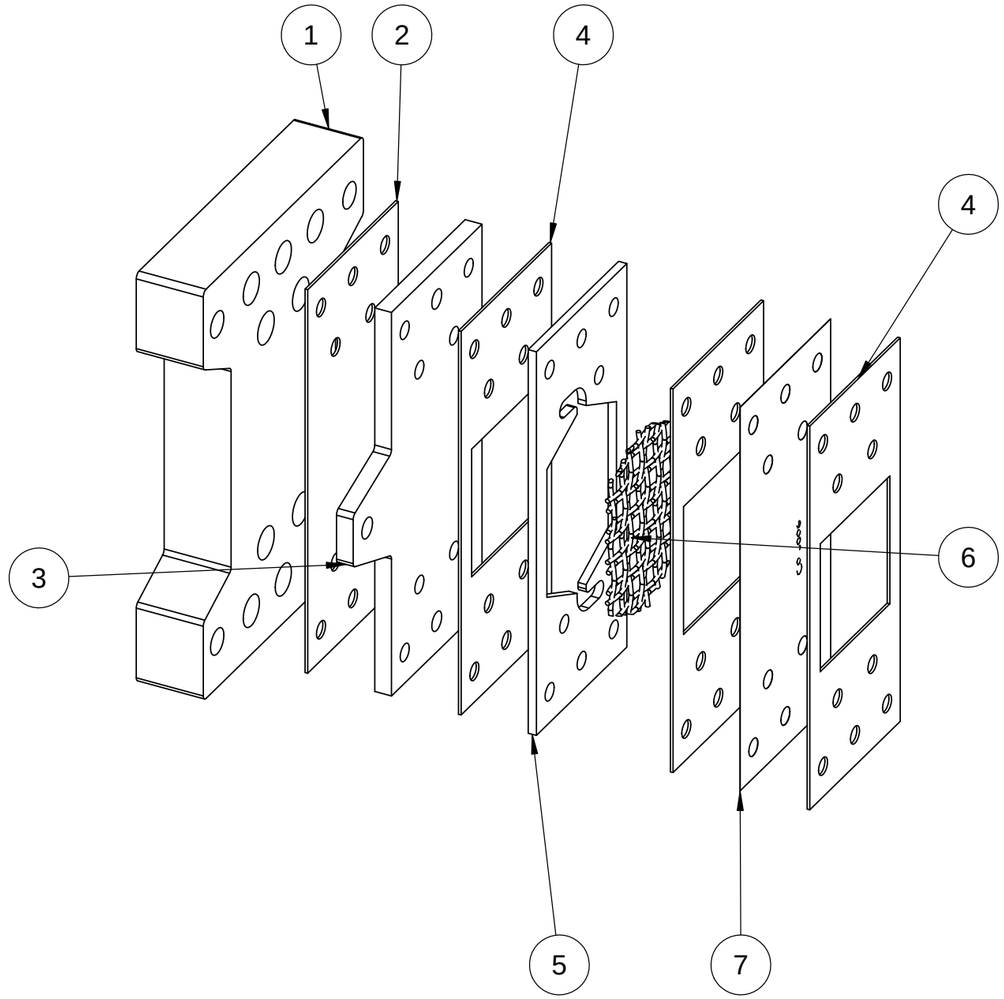

ITEM NO.	PART NUMBER	QTY.
1	BMED End Plate	1
2	Full Gasket	1
3	BMED Full Side Electrode	1
4	Open Gasket	3
5	Rinse	1
6	Woven Flow Spacer	1
7	Bipolar Membrane	1

Project: Electrodialysis / Bipolar-membrane Electrodialysis Stack		
Title: ED / BMED Stack Components		
Subtitle: Cathode Assembly		
Drawn by: David Saabas	**Date:** Jan 13 2021	
Units: All dimensions in mm	Appendix B Drawing 11 of 12	
Sheet Size: 11" x 17"	**Sheet Scale:** 1:1	**Revision:** 1

2 Compartment BMED Repeating Unit

ITEM NO.	PART NUMBER	QTY.
1	Raw or Product	2
2	Woven Flow Spacer	2
3	Open Gasket	4
4	Cationic Membrane	1
5	Bipolar Membrane	1

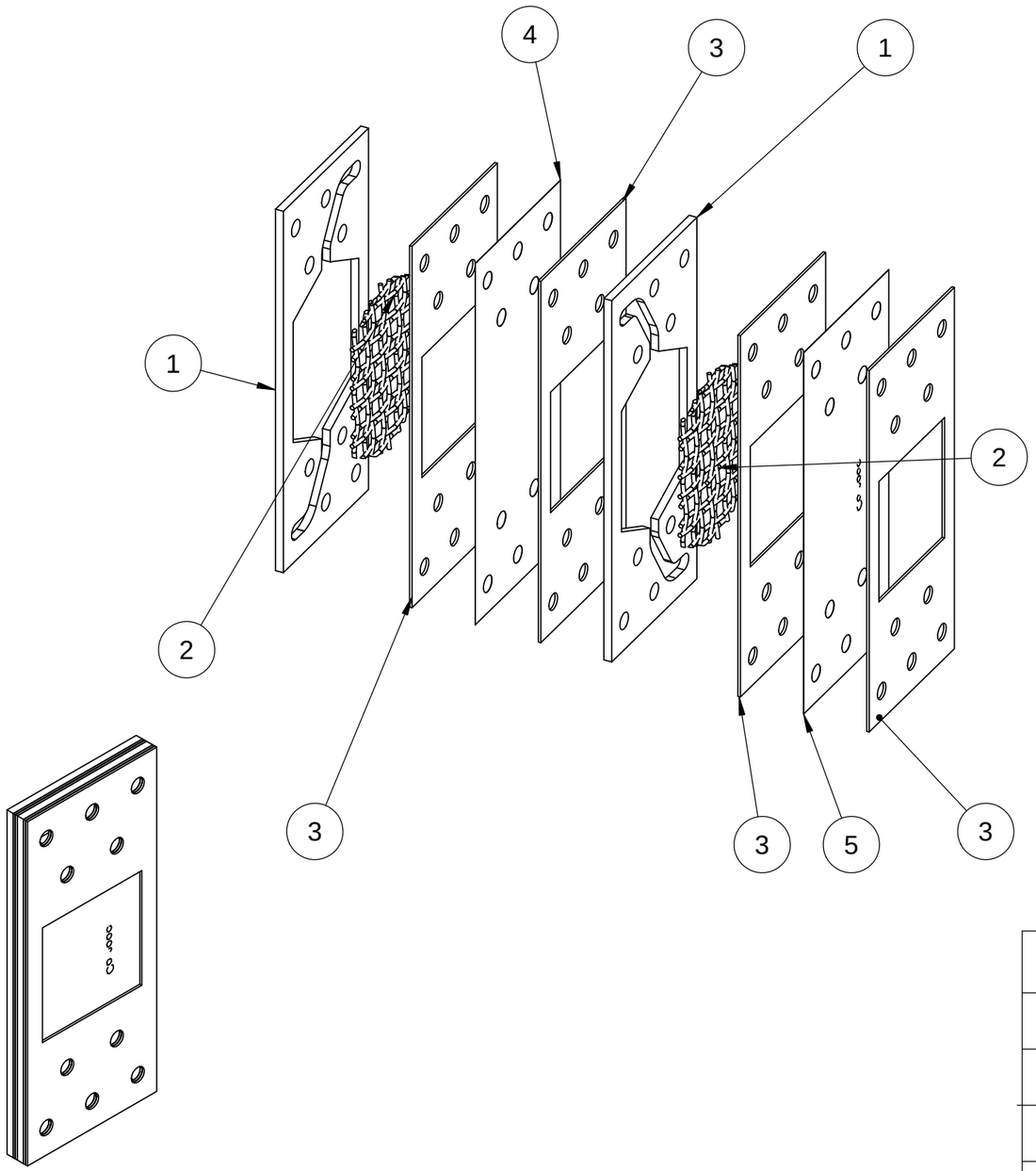

Repeating Units can be added in series, typically three are used

Note the alternating pattern of the Raw or Product Spacer

Project: Electrodialysis / Bipolar-membrane Electrodialysis Stack		
Title: ED / BMED Stack Components		
Subtitle: 2 Compartment BMED repeating unit for stack		
Drawn by: David Saabas	**Date:** Jan 13 2021	
Units: All dimensions in mm	Appendix B Drawing 12 of 12	
Sheet Size: 11" x 17"	**Sheet Scale:** 1:1	**Revision:** 1